Modeling spinal muscular atrophy in *Drosophila* links *Smn* to FGF signaling

Anindya Sen,[1] Takakazu Yokokura,[1] Mark W. Kankel,[1] Douglas N. Dimlich,[1] Jan Manent,[1] Subhabrata Sanyal,[2] and Spyros Artavanis-Tsakonas[1,3]

[1]Department of Cell Biology, Harvard Medical School, Boston, MA 02115
[2]Department of Cell Biology, Emory University, Atlanta, GA 30322
[3]Collège de France, Paris 75005, France

Spinal muscular atrophy (SMA), a devastating neurodegenerative disorder characterized by motor neuron loss and muscle atrophy, has been linked to mutations in the *Survival Motor Neuron* (*SMN*) gene. Based on an SMA model we developed in *Drosophila*, which displays features that are analogous to the human pathology and vertebrate SMA models, we functionally linked the fibroblast growth factor (FGF) signaling pathway to the *Drosophila* homologue of *SMN*, *Smn*. Here, we characterize this relationship and demonstrate that *Smn* activity regulates the expression of FGF signaling components and thus FGF signaling. Furthermore, we show that alterations in FGF signaling activity are able to modify the neuromuscular junction defects caused by loss of *Smn* function and that muscle-specific activation of FGF is sufficient to rescue *Smn*-associated abnormalities.

Introduction

Spinal muscular atrophy (SMA) is an inherited neurodegenerative disease causing progressive deterioration of motor functions and loss of motor neurons (Azzouz et al., 2004). After cystic fibrosis, SMA is the most common autosomal recessive disorder in humans with an incidence of 1 in 6,000 and defines the most common genetic cause of infant mortality. SMA is caused by the loss of *Survival Motor Neuron* (*SMN1*), a ubiquitously expressed gene that encodes a key component of the SMN complex, which is essential for snRNP biogenesis. Biochemical studies established that SMN mediates the accuracy of interactions between RNA binding proteins and their target snRNAs in the cytoplasm (Massenet et al., 2002; Meister et al., 2002; Paushkin et al., 2002; Wan et al., 2005; Battle et al., 2006; Eggert et al., 2006; Zhang et al., 2008).

The human genome harbors two homologous, nearly identical genes encoding SMN, *SMN1*, and *SMN2*. However, under normal conditions, *SMN1* accounts for 90% of cellular SMN expression due to a splicing mutation in *SMN2* that results in the production of only a small fraction (~10%) of full-length functional SMN (Lefebvre et al., 1997; Wolstencroft et al., 2005). Thus, though SMA is caused by mutations that impair *SMN1* function, the severity of the disease is modulated by *SMN2* copy number, which varies in the human population (McAndrew et al., 1997). As *SMN2* copy number increases, the amount of full-length SMN protein also increases, rendering loss of *SMN1* less pathogenic. Therefore, cellular processes as well as single genes capable of augmenting SMN protein activity may be therapeutically relevant. To identify such processes/targets and gain insights into fundamental aspects of SMA, several different organisms, including *Drosophila*, are currently being used to model this disease (Schrank et al., 1997; Miguel-Aliaga et al., 1999, 2000; Frugier et al., 2000; Hannus et al., 2000; Hsieh-Li et al., 2000; Monani et al., 2000; Owen et al., 2000; Paushkin et al., 2000; Chan et al., 2003; McWhorter et al., 2003; Rajendra et al., 2007; Chang et al., 2008; Briese et al., 2009; Kong et al., 2009).

The *Drosophila* genome encodes a single orthologue of SMN, the Survival motor neuron (Smn) protein, which is ubiquitously expressed and localizes to nuclear gems (Chan et al., 2003; Liu et al., 2006; Chang et al., 2008), similar to the distribution observed in vertebrates (Monani, 2005). In *Drosophila*, *Smn*

A. Sen, T. Yokokura, and M.W. Kankel contributed equally to this paper.

Correspondence to Spyros Artavanis-Tsakonas: artavanis@hms.harvard.edu

Abbreviations used in this paper: *btl*, *breathless*; *htl*, *heartless*; EJP, excitatory junction potential; MSA, muscle surface area; NMJ, neuromuscular junction; SMA, spinal muscular atrophy; SMN, Survival Motor Neuron; *sty*, *sprouty*.

The Rockefeller University Press $30.00
J. Cell Biol. Vol. 192 No. 3 481–495
www.jcb.org/cgi/doi/10.1083/jcb.201004016

loss-of-function mutations result in reduced viability and decreased motility as well as muscular atrophy in the adult thorax, phenotypes analogous to the human pathology (Chan et al., 2003; Rajendra et al., 2007; Chang et al., 2008). Moreover, neuromuscular junction (NMJ) defects are associated with both vertebrate and invertebrate models (Chan et al., 2003; Chang et al., 2008; Kariya et al., 2008). In addition to its canonical subcellular distribution, Smn is also clearly concentrated in the postsynaptic region of the larval NMJ (Chang et al., 2008) and has been reported to localize to sarcomeres of adult myofibrils (Rajendra et al., 2007). Despite this, tissue-specific reduction of Smn demonstrates that normal NMJ morphology requires *Smn* activity in both muscles and neurons (Chang et al., 2008). Finally, an observation of critical importance to the *Drosophila* model is that the morphology and the physiology of the NMJ are sensitive to levels of Smn (Chang et al., 2008; unpublished data), mirroring the *SMN2* dosage dependence observed in SMA patients.

Taking advantage of the dosage sensitivity of *Smn* loss-of-function phenotypes, we performed systematic genetic screens to identify modifiers of *Smn* activity (Chang et al., 2008). Among the genes identified in this manner was the *breathless* locus, which encodes one of the two *Drosophila* FGF receptors (Glazer and Shilo, 1991). In general, the FGF pathway has been demonstrated to be involved in a diverse range of cellular and developmental processes, including proliferation, migration, differentiation, and apoptosis (Itoh and Ornitz, 2004; Huang and Stern, 2005). In *Drosophila*, this pathway has been demonstrated to control the development of the tracheal system (Ghabrial et al., 2003) and the musculature (Shishido et al., 1993, 1997; Beiman et al., 1996; Gisselbrecht et al., 1996; Michelson et al., 1998; Vincent et al., 1998; Schulz and Gajewski, 1999; Stathopoulos et al., 2004). In contrast, the role of FGF in the *Drosophila* nervous system remains poorly characterized (García-Alonso et al., 2000; Forni et al., 2004).

In this study, we investigate the relationship between *Smn* and several components of the FGF pathway, demonstrating a clear link between *Smn* and FGF. Epistasis analysis reveals that *Smn* regulates FGF signaling output, and molecular studies indicate that *Smn* activity influences FGF receptor transcript levels. Furthermore, we show that activation of FGF signaling can restore *Smn*-associated NMJ defects, thus raising the possibility that FGF can act as a protective modifier of SMA.

Results

The FGF signaling pathway and *Smn*

breathless (*btl*), which encodes one of the two known *Drosophila* FGF receptors, was identified in a genetic screen as a modifier of *Smn*-dependent lethality (Chang et al., 2008), suggesting a connection between the FGF pathway (Fig. 1 A) and *Smn*. We extended this finding by determining the effect of different *btl* mutations on *Smn*-dependent viability using an inducible RNAi allele of *Smn*, *UAS-Smn-RNAi*^{FL26B} (FL26B), which displays reduced viability when ubiquitously expressed by the *tubulinGAL4* (*tubGAL4*) driver (Chang et al., 2008). This phenotype was modified by multiple *btl* alleles (*btl*^{f02864}, *btl*^{dev1}, and *UAS-λbtl*) as judged by our survival assay (Fig. S1, A and B). These genetic results confirm *btl* as a bona fide modifier of *Smn* loss-of-function mutations, thereby validating our initial observations.

If, as the above analysis of *btl* implies, FGF signaling can modulate *Smn* activity, we expect other genetic elements of the FGF pathway to behave as *Smn* modifiers as well. We chose to examine this relationship in the mesoderm, as the activity of the FGF signaling pathway has been shown to be important for the development and the maintenance of muscles (Shishido et al., 1993; Beiman et al., 1996; Gisselbrecht et al., 1996; Michelson et al., 1998; Vincent et al., 1998; Schulz and Gajewski, 1999; Stathopoulos et al., 2004). The mesoderm-specific *how24BGAL4* driver was used to control expression of inducible RNAi transgenes that specifically target either of the two *Drosophila* FGF receptors, *btl* or *heartless* (*htl*), and a specific FGF signaling effector, *stumps*. We monitored the effects of these mutations on two additional *Smn* RNAi strains, *UAS-Smn-RNAi*^{C24} (C24) and *UAS-Smn-RNAi*^{N4} (N4), which, based on phenotypic analyses and Smn expression levels, are of increasing allelic strength with respect to the FL26B allele (Chang et al., 2008).

In control experiments, we observe an *Smn*-independent effect on viability in backgrounds in which Btl, Htl, or Stumps expression were reduced, whereas no effect on viability was observed upon removal of one copy of *sprouty* (*sty*), an inhibitor of the pathway (Fig. 1, B and C). However, when *Smn* activity is reduced in each of these backgrounds, a further decrease in viability is detected (Fig. 1, B and C). Moreover, loss of function for the FGF pathway antagonist *sty* suppresses *Smn*-induced lethality (Fig. 1 C). Based on these observations, we conclude that a genetic link between *Smn* activity and the FGF signaling cascade exists in the mesoderm.

Reduction of FGF signaling in muscles causes NMJ defects

Previous analyses established that the vast majority of mutations in genes that altered the viability of *Smn* loss-of-function mutations (Chang et al., 2008) were also accompanied by structural defects in the larval NMJ (Chang et al., 2008). As multiple alleles of several FGF signaling elements modify *Smn*-dependent lethality, we assessed the significance of this interaction at the third larval instar NMJ in several different genetic backgrounds.

An initial examination of the distribution of Htl revealed that it is specifically expressed at the NMJ during the third instar (Fig. 2, A–L; and Fig. S2). This expression appears to be primarily in the muscle, as it coincides with the postsynaptic marker Discs Large 1 (Dlg; Fig. 2 B) and does not obviously overlap with the presynaptic marker nc82 (Bruchpilot; Fig. 2 E). This is corroborated by the localization of additional presynaptic markers, Cysteine string protein (Csp; Fig. 2 H) and anti-horseradish peroxidase (anti-HRP; Fig. 2 K), which label synaptic vesicles and neuronal membranes, respectively, and appear to be distinct from Htl expression. Together, these data suggest that Htl is predominantly postsynaptic, as indeed is Smn.

The presence of the *htl* ligands, *pyramus* (*pyr*) and *thisbe* (*ths*) at the NMJ would suggest that Htl is active, but the localization of the ligands has not been previously described. In embryos, it is known that the ligands are expressed in the epithelia adjacent to the mesoderm, which expresses *htl*

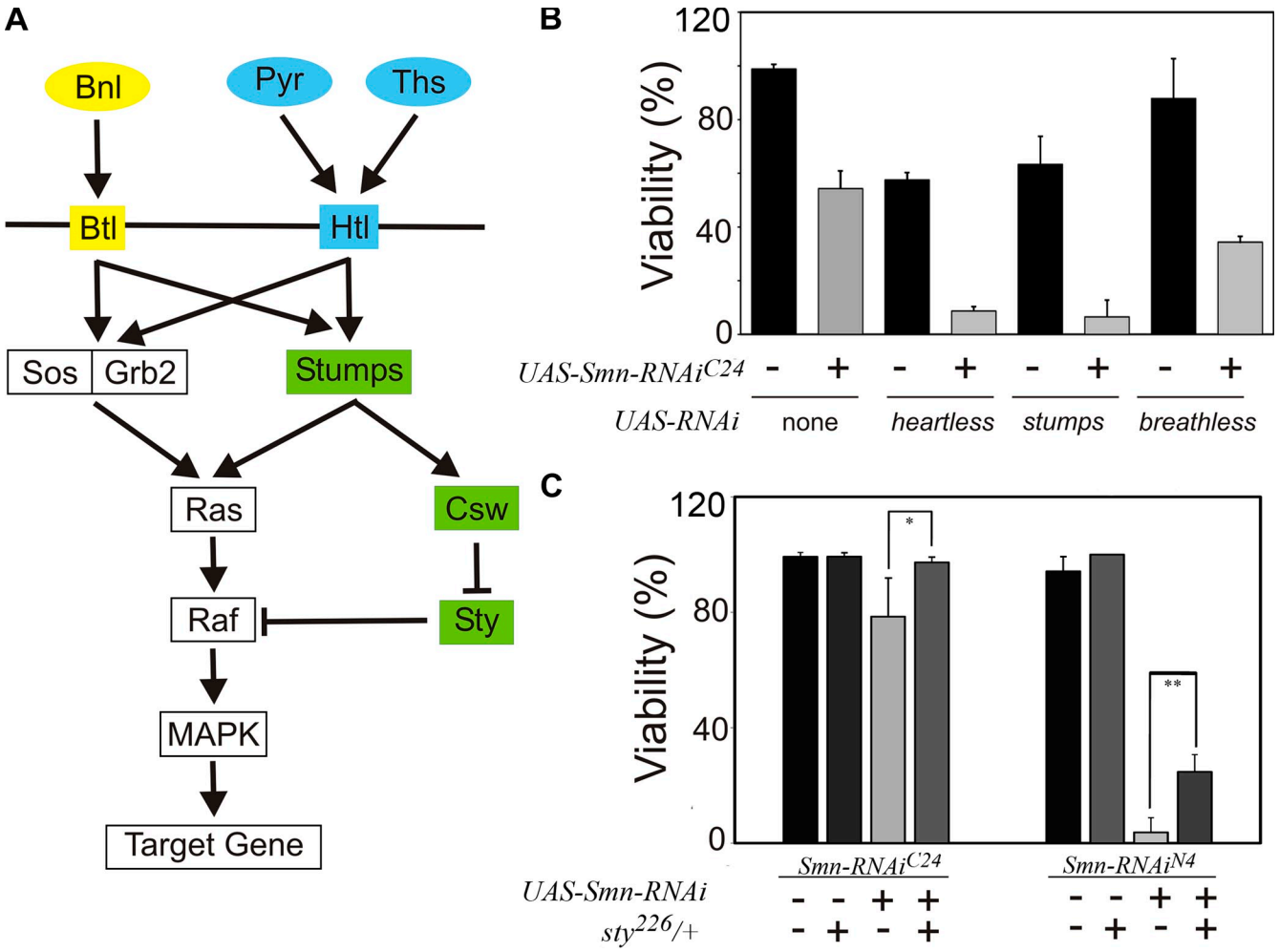

Figure 1. **Multiple FGF pathway components modify *Smn*-dependent viability.** (A) Schematic diagram depicting the FGF signaling pathway in *Drosophila*. In *Drosophila*, pathway activation is mediated by the two known FGF receptor orthologues, *breathless* (*btl*) and *heartless* (*htl*) (Glazer and Shilo, 1991). *btl*, which functions in the tracheal system, is activated by its ligand *branchless* (*bnl*) (Sutherland et al., 1996), whereas *htl*, which functions in the mesoderm and muscles, is activated either by the *thisbe* (*ths*) (Kerr et al., 2003) or *pyramus* (*pyr*) (Stathopoulos et al., 2004) ligands. Both receptors act through Sos-Grb2 to activate Ras/Raf/MAP kinase signaling. Additional regulation of Ras/Raf/MAP kinase signaling occurs through *stumps* (Vincent et al., 1998), which regulates the phosphatase *corkscrew* (*csw*) (Petit et al., 2004). In turn, Csw negatively regulates *sprouty* (*sty*), itself a negative regulator of Raf, thereby leading to MAPK activation (Jarvis et al., 2006). (B) The lethal phenotype associated with mesoderm-specific *how24BGAL4*-directed expression of *UAS-Smn-RNAi*^{C24} is enhanced by the reduction of the FGF signaling pathway components *htl*, *stumps*, and *breathless*. (C) *sprouty* alleles suppress the *how24BGAL4 UAS-Smn-RNAi* lethal phenotype. Significant differences are indicated (*, $P < 0.05$; **, $P < 0.01$).

(Stathopoulos, et al., 2004). However, because antibodies that recognize the ligands are not available, we used qPCR to determine that each is expressed to varying degrees in the third instar larva (Fig. 2, M and N).

Although the above analysis is compatible with the notion that the postsynaptic expression of Htl is functionally relevant, it does not have the resolution necessary to provide reliable evidence for Htl activity. To explore this possibility directly, we examined the NMJs of larvae in which *htl* activity is reduced through the muscle-directed expression of an *htl* dominant-negative transgenic construct (*how24BGAL4/UAS-htl*^{DN}; Michelson et al., 1998). This manipulation caused significant alterations in the NMJ synaptic terminals (Fig. 3 B) as compared with sibling controls (Fig. 3 A). The defects were quantified by counting the number of boutons per muscle and normalized to muscle surface area, revealing a significant (~40%) reduction in synaptic size (Fig. 3 G and Fig. S3 A).

To corroborate these observations and ensure that the structural defects we observe at the larval NMJ are associated with the FGF pathway, we modulated the activities of *htl* and its downstream effectors, *stumps* (*dof*) and *sprouty* (*sty*) using GAL4-inducible transgenic strains to determine whether further modifications in FGF signaling result in structural defects at the larval NMJ. Muscle-specific expression of *sty*, a dominant inhibitor of the pathway (*how24BGAL4:UAS-sty*; Fig. 3, C and G; and Fig. S3 A), or a transgenic *UAS-htl* RNAi construct caused a similar NMJ phenotype (*how24BGAL4:UAS-htl*-RNAi; Fig. 3 G and Fig. S3 A).

Though overexpression of just *htl* in muscles had no discernable impact on NMJ growth (*how24BGAL4:UAS-htl*; Fig. 3 G and Fig. S3 A), expression of *stumps*, which acts upstream of Ras, caused a pronounced synaptic overgrowth and an overelaboration of synaptic terminals (*how24BGAL4:UAS-stumps*; Fig. 3, D and G; and Fig. S3 A). Quantification of the number of synaptic boutons,

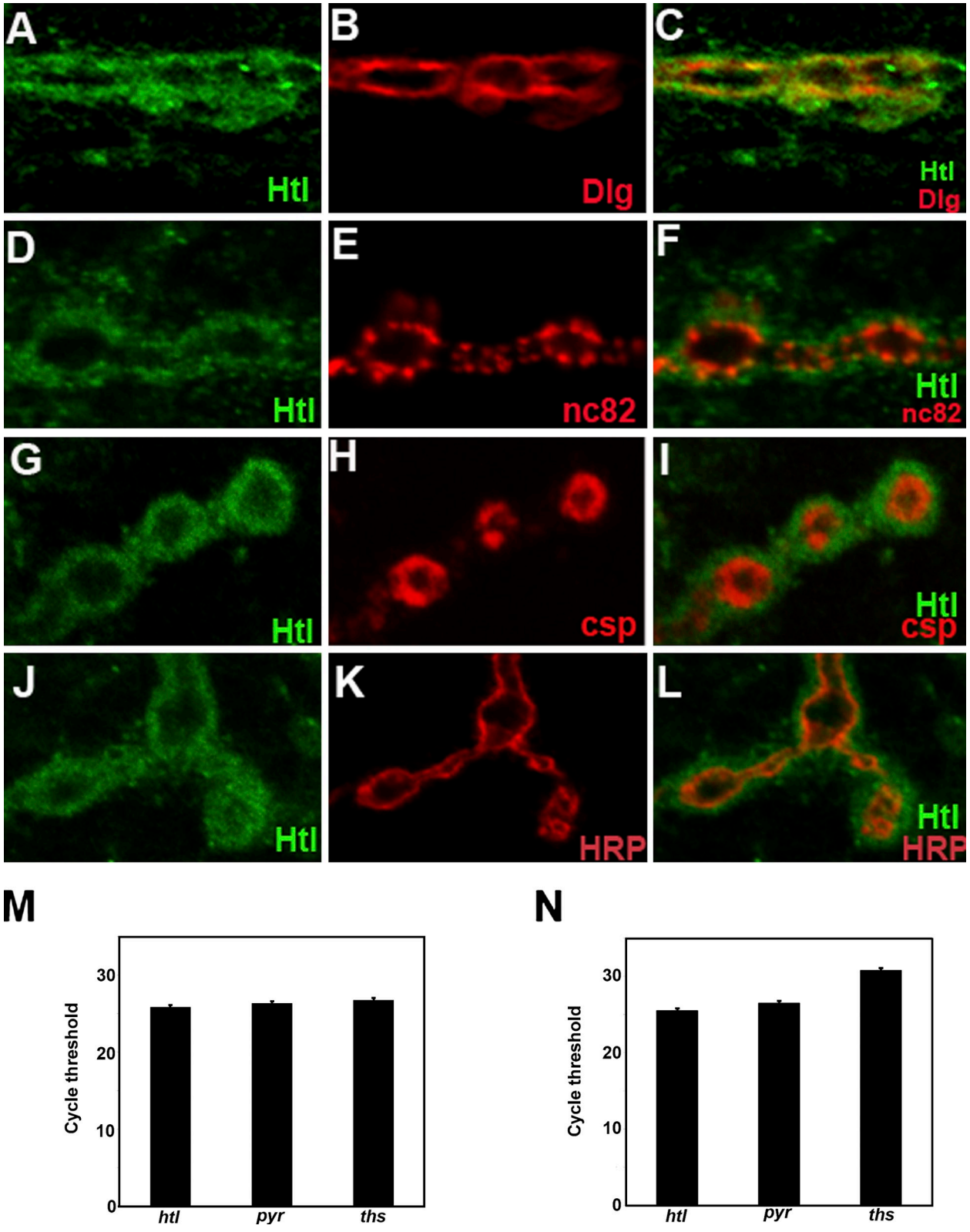

Figure 2. **Heartless localizes to the postsynaptic region of the *Drosophila* larval NMJ.** All panels show wild-type NMJs derived from larval muscle 4. (A, D, G, and J) Htl (green) expression in the NMJ boutons. (B) Dlg (red) marks the postsynaptic region of the NMJ. (C) Htl (green) and Dlg (red) expression coincide at the larval NMJ. (F) Htl (green) and the presynaptic nc82 (red) expression do not overlap at the NMJ boutons. (I) Mutually exclusive expression of Htl (green) and presynaptic marker Csp (red) at the larval NMJ. (L) Htl (green) expression does not colocalize with presynaptic HRP staining (red). (M and N) qPCR from mRNA derived from tissues extracted from third instar larvae reveals the expression of *htl* and its ligands, *ths* and *pyr*, in the brain (M) and muscle (N). Bar, 5 µm.

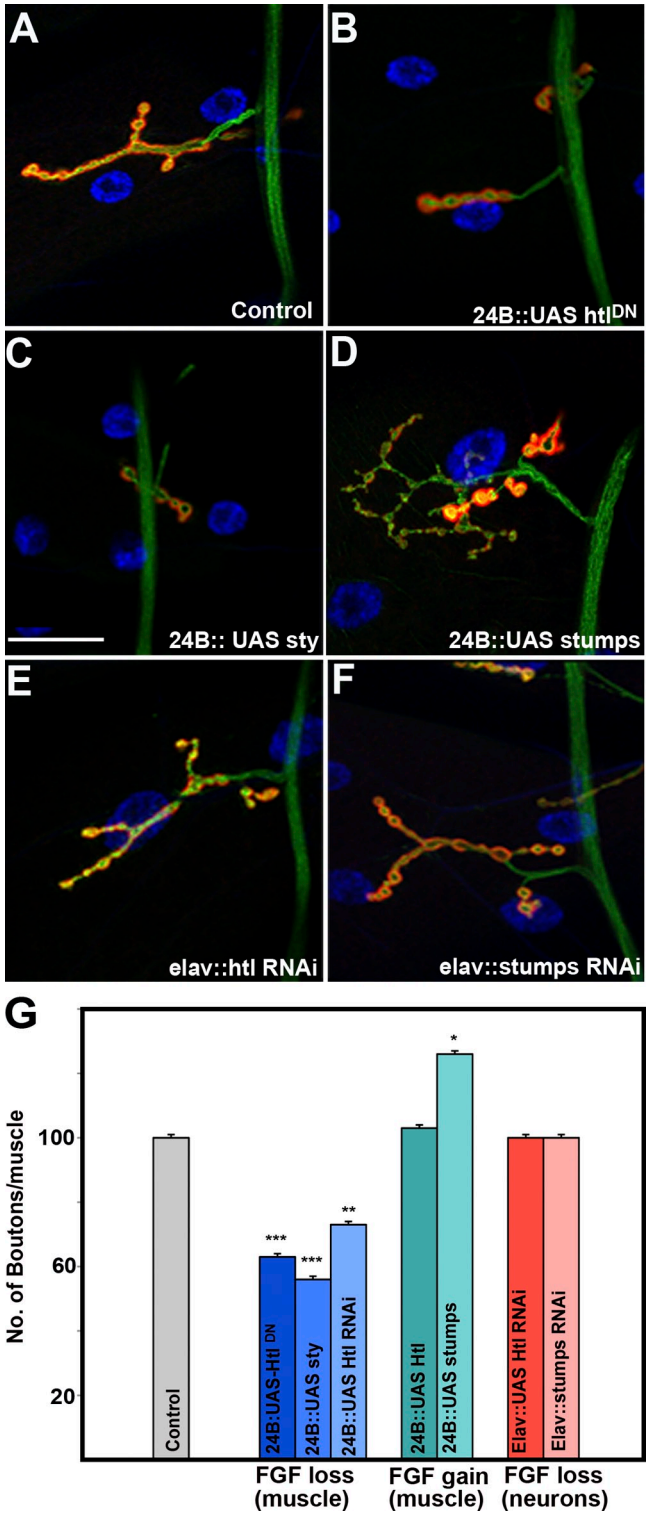

Figure 3. ***heartless* signaling regulates NMJ morphology.** (A) Wild-type NMJ derived from larval muscle 4. (B) Drastic reduction in NMJ size in *how24BGAL4* animals driving expression of a transgenic construct carrying a dominant-negative *heartless* (*UAS-htl*^{DN}). The *how24BGAL4* driver expresses GAL4 predominantly in the muscles. (C) Reduction in NMJ size by overexpression of Sprouty. (D) Expansion of the NMJ in animals overexpressing Stumps by *how24BGAL4*. (E) Neuronal overexpression of *htl* RNAi by *elavGAL4* has no effect on NMJ size or morphology. (F) Neuronal overexpression of *stumps* RNAi has no effect on NMJ size and/or morphology. (G) Quantitation of bouton number/muscle in animals of the indicated genotypes, normalized to muscle surface area (MSA) as a percentage of wild type (WT). *how24BGAL4/+* animals are used as controls. The ANOVA multiple comparison test was used for statistical analysis of the bouton number/muscle. $P \leq 0.05$. Bar, 50 µm. $n = 40$.

which reflects synaptic size, revealed that muscle-specific *stumps* overexpression resulted in a 15–20% increase in the number of synaptic boutons at muscle 4 (Fig. 3 G and Fig. S3 A) and a 35% increase at the muscle 6/7 A3 synapse (Fig. S4) relative to controls. Though there was a significant effect on NMJ size, there were no gross morphological defects as the localization of pre- (anti-HRP) and postsynaptic markers (anti-Dlg) were not detectably altered, and there was no major variation in muscle size or morphology. Thus, the effects of FGF loss-of-function (Fig. 3, B, C, and G; and Fig. S3 A) are opposite to those observed for FGF gain-of-function (Fig. 3, D and G; and Fig. S3 A) in the regulation of synaptic elaboration on muscle 4, a strong genetic argument in favor of a functional role for FGF signaling at the NMJ.

In contrast, presynaptic expression of RNAi transgenes for *htl* and *stumps* using the *elavGAL4* driver did not result in any measurable changes in synaptic size (*elavGAL4:UAS-htl* or *elavGAL4:UAS-stumps*; Fig. 3, E–G; and Fig. S3 A), suggesting that *htl* and *stumps* are not active presynaptically. It is important to point out, however, that we cannot exclude a presynaptic role for these elements of the FGF pathway given the possibility that RNAi in neurons may not have been effective. Despite this caveat, these experiments demonstrate that activation of the FGF pathway in the muscle is required to regulate the size of the NMJ.

FGF signaling in muscles affects responsiveness to presynaptic transmitter release

The preceding experiments show that altering FGF components in the muscle influences presynaptic morphology, which is likely accompanied by changes in either transmitter release or postsynaptic receptivity. To directly test this possibility, we performed electrophysiological measurements of evoked excitatory junction potentials (EJPs) under conditions in which we either increased or decreased FGF signaling selectively in the muscle using the *how24BGAL4* driver. Perturbation of FGF signaling in muscles primarily leads to altered mEJP (miniature EJP) amplitude or quantal size (Fig. 4), a phenotype most often associated with the postsynaptic compartment (Petersen et al., 1997). Thus, increasing the expression of wild-type Htl decreases the average mEJP amplitude by more than 50%, whereas inhibition of FGF signaling through expression of the dominant-negative *htl* transgene increases mEJP amplitude by 50%. Interestingly, such reciprocal regulation of quantal size by *htl* is also mirrored in our EJP measurements (Fig. 4, A and B). As a result, quantal content (defined as the number of synaptic vesicles released per action potential and estimated by dividing the mean EJP response by the mean mEJP amplitude) remains essentially unchanged across genotypes. In addition, there are no observed changes in the frequencies of spontaneous release. It is noteworthy that changes in EJP and mEJP values are contrary to those observed for presynaptic bouton number, an observation most parsimoniously explained through feedback mechanisms

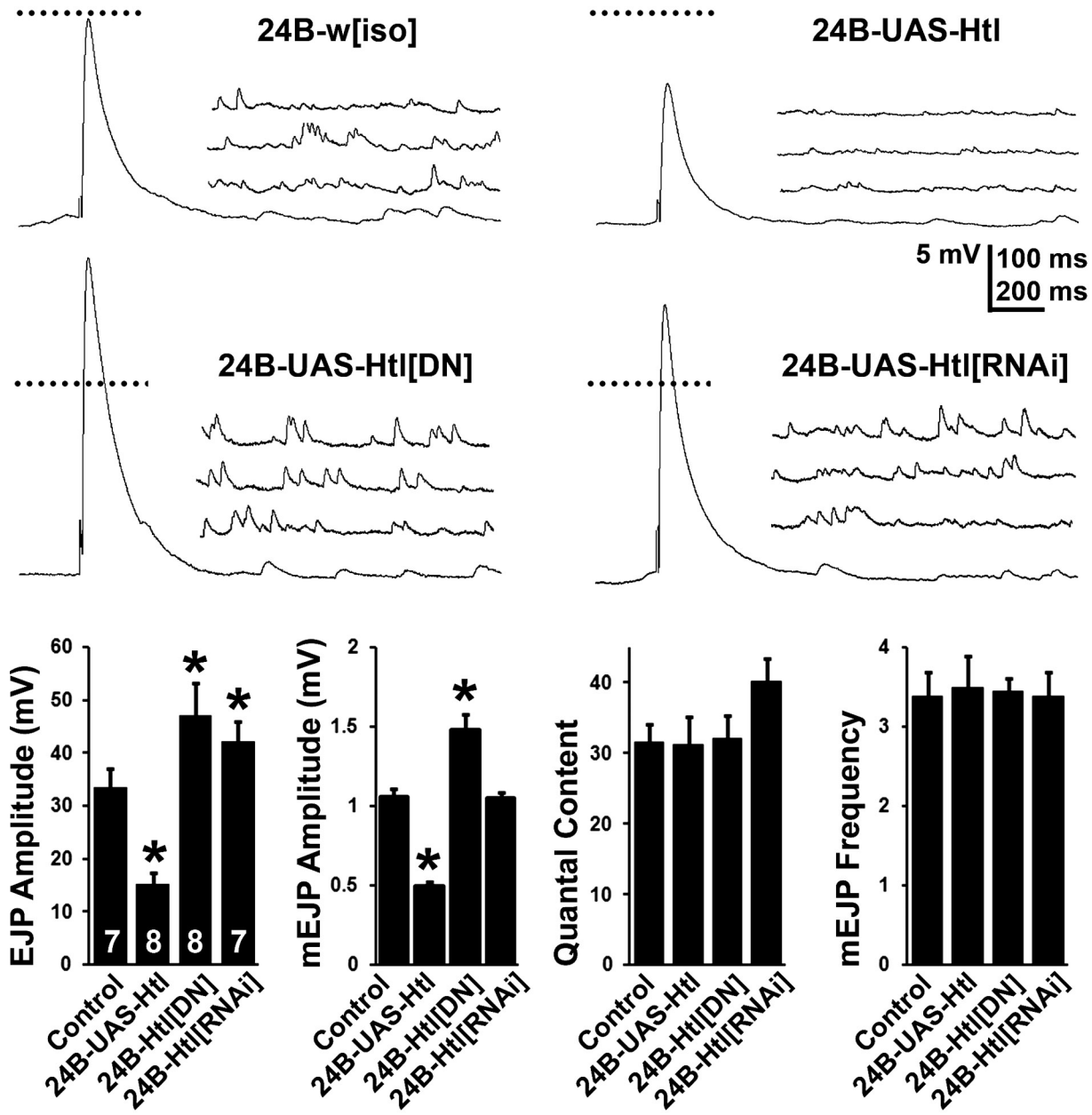

Figure 4. **Postsynaptic FGF signaling regulates the quantal size of transmitter release.** (top) Representative recordings of EJP and mEJP at 0.5 mM extracellular Ca^{2+} are shown for control (*how24BGAL4-w*[iso]), muscle expression of wild-type Htl (*how24BGAL4-UAS-htl*), muscle expression of a Htl dominant-negative Htl (*how24BGAL4-UAS-htl*[DN]), and muscle expression of an RNAi targeted against Htl (*how24BGAL4-UAS-htl*[RNAi]). Whereas Htl expression reduces both EJP and mEJP amplitude, Htl inhibition leads to significantly larger EJP and mEJP amplitudes. Horizontal scale bar is 100 ms for EJPs and 200 ms for mEJPs. Dotted line represents magnitude of control EJP. (bottom) Quantification of EJP amplitude, mEJP amplitude, quantal content, and mEJP frequency in the four genotypes. Both EJP and mEJP amplitude are altered after experimental perturbation in Htl signaling in the muscle. Quantal content of transmitter release, however, remains unchanged. Similarly, the frequency of spontaneous release is comparable across genotypes. Asterisks denote $P < 0.01$ (ANOVA). The number of animals recorded for each genotype is shown within the first graph.

that are known to operate at the larval NMJ to control its structural and functional properties (see Discussion). Therefore, the morphological changes associated with FGF signal modulation at the NMJ are accompanied by functional abnormalities.

Synergy of *Smn* and FGF signaling in muscles regulates NMJ growth

Given that the effects of loss of FGF signaling on NMJ morphology are independent of *Smn*, it is possible that the observed interactions between this pathway and *Smn* arise from the cumulative, rather than synergistic, effects of these mutations. If these interactions were due to additive effects, then the introduction of a single recessive allele of either *btl* or *htl* would not be expected to significantly alter the NMJ phenotype of *Smn* mutants. Therefore, we assayed whether either a strong hypomorphic allele of *btl* (*btl*^{dev1}) or a null allele of *htl* (*htl*^{AB42}) could modify as heterozygotes the reduction of the NMJ size caused by the muscle-specific expression of the *UAS-Smn-RNAi*^{C24} allele.

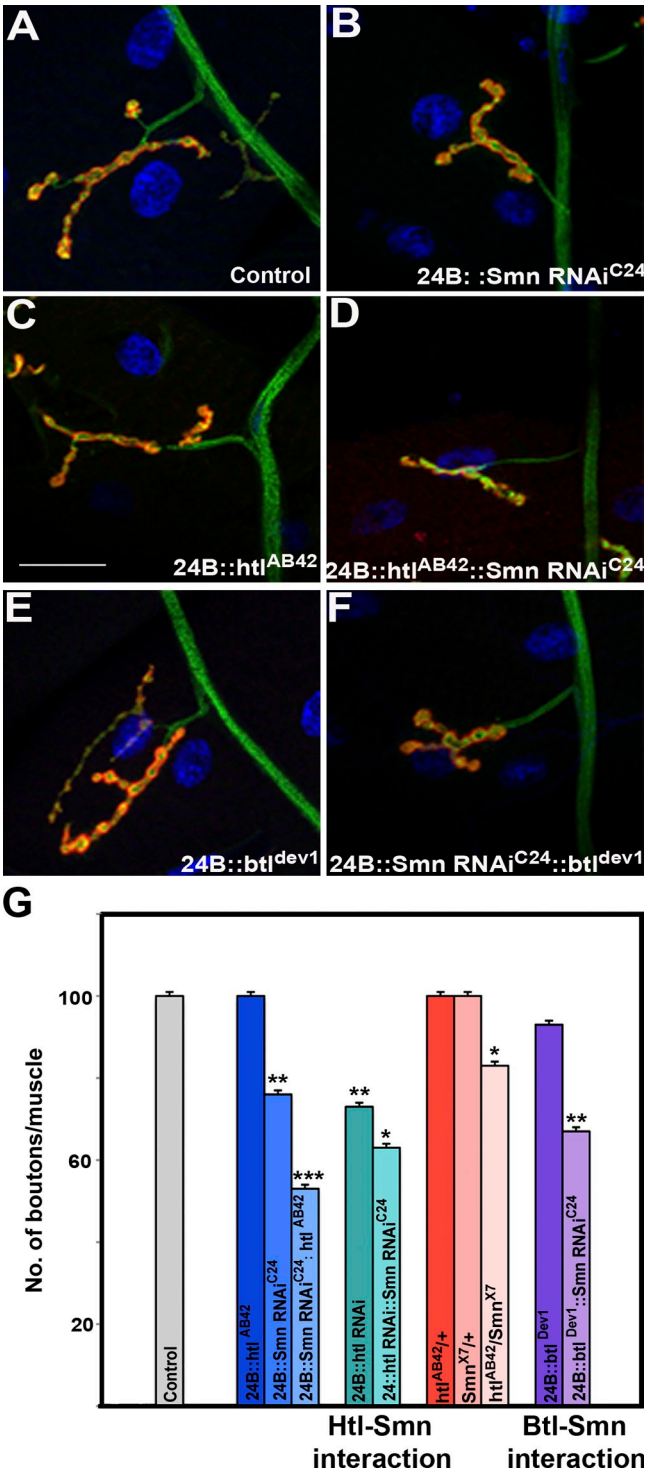

Figure 5. **Synergy between *Smn* and FGF signaling regulates NMJ morphology.** (A) Wild-type NMJ derived from larval muscle 4. *how24BGAL4* expresses GAL4 predominantly in the mesoderm (muscles). (B) Reduction in NMJ size resulting from muscle-specific (*how24BGAL4*) reduction of *Smn* (*UAS-Smn-RNAi*^{C24}). (C) Heterozygotes carrying the null allele *htl*^{AB42} show no effect on the number of synaptic boutons. (D) Reduction in NMJ size in *how24BGAL4 UAS-Smn-RNAi*^{C24}*/htl*^{AB42}. (E) *how24BGAL4; btl*^{dev1}*/+* animals do not show any significant effects on the NMJ. (F) *how24BGAL4 UAS-Smn-RNAi*^{C24}*/btl*^{dev1} transheterozygous animals have reduced synapses. (G) Quantitation of bouton number/muscle in animals of indicated genotypes, normalized per muscle surface area (MSA) as a percentage of wild type (WT). *how24BGAL4/+* is used as control. The ANOVA multiple comparison test was used for statistical analysis of the bouton number/muscle. $P \leq 0.05$. Bar, 50 µm. $n = 40$. All preparations were stained with anti-HRP (red) and anti-Dlg (green). The muscle nucleus was labeled using DAPI.

Examination of larvae heterozygous for either of the two FGF receptors (*how24BGAL4/btl*^{dev1} or *how24BGAL4/htl*^{AB42}) revealed the introduction of these mutations had no significant effect on the NMJ size of animals from the *how24BGAL4* driver genetic background (*how24BGAL4/+*) as assayed by the number of synaptic boutons per unit of muscle surface area (MSA; Fig. 5, A, C, E, and G; and Fig. S3 B). In contrast, when *Smn* function is reduced by the introduction of the *UAS-Smn-RNAi*^{C24} allele into these genetic backgrounds (*how24BGAL4 UAS-Smn-RNAi*^{C24}*/btl*^{dev1} and *how24BGAL4 UAS-Smn-RNAi*^{C24}*/htl*^{AB42}), these heterozygous FGF receptor mutations elicited a drastic decrease in synaptic size when compared with loss of *Smn* alone (*how24BGAL4 UAS-Smn-RNAi*^{C24}*/+*; Fig. 5, B, D, and G; and Fig. S3 B).

Because these results indicate the link between FGF signaling and *Smn* activity is synergistic rather than additive, we applied a further, more stringent assay to determine the sensitivity of the NMJ to this interaction. Examination of transheterozygous larvae carrying a combination of null alleles of *Smn* and *htl* (*Smn*^{X7}*/htl*^{AB42}) revealed that simultaneously reducing the dosage of each locus by half leads to a statistically significant decrease in the number of synaptic boutons per unit MSA when compared with each heterozygote alone (*Smn*^{X7}*/+* and *+/htl*^{AB42}; Fig. 5 G and Fig. S3 B). Thus, this experiment provides formal evidence that the relationship we have uncovered is synergistic in nature and is not merely due to the additive effects of two mutations that independently affect the NMJ.

Activation of FGF signaling in muscles rescues synaptic defects caused by *Smn* RNAi

Because reduction of FGF signaling clearly exacerbates the NMJ defects caused by *Smn* loss, we examined whether activation of this pathway could reverse these effects. As shown in Fig. 6, muscle-specific overexpression of wild-type Htl completely rescues the NMJ phenotypes associated with both the *UAS-Smn-RNAi*^{C24} allele and the stronger *UAS-Smn-RNAi*^{N4} allele (Fig. 6, B–D and G; Fig. S3 C). In control crosses, expression of Stumps alone resulted in an expansion of synaptic branching (Fig. 6 E); however, as observed for Htl, expression of Stumps completely suppressed the NMJ defects observed in the *how24BGAL4*; *UAS-Smn-RNAi*^{C24} background (Fig. 6 F and G; and Fig. S3 C). These results suggest that *Smn* is situated upstream of the FGF pathway. Based on this genetic behavior, however, we could not distinguish whether *Smn* directly regulates *htl* or any other pathway component.

Smn regulates expression of the FGF receptor, Htl, and its downstream effector Stumps

To further explore the relationship between *Smn* and FGF signaling pathway components, we first tested whether reducing *Smn*

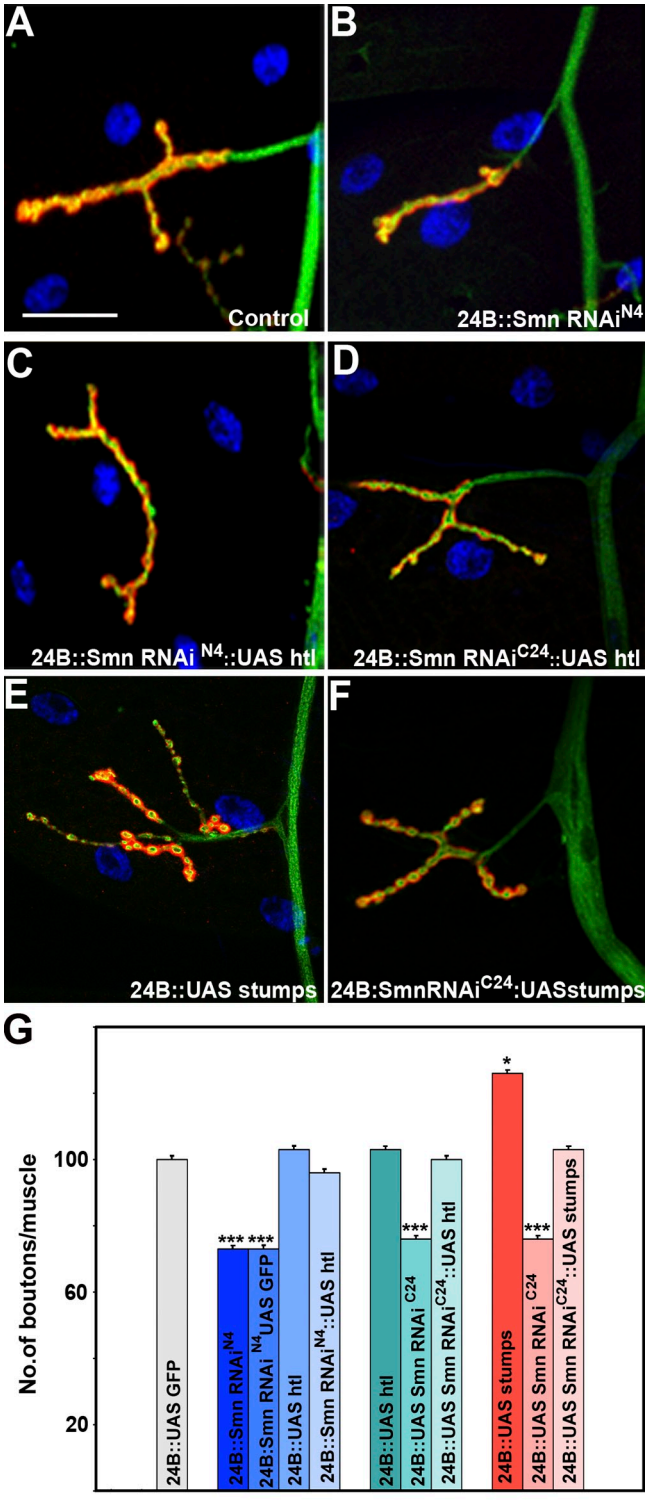

Figure 6. **Overexpression of Htl rescues NMJ defects caused by reduced Smn.** *how24BGAL4* expresses GAL4 predominantly in the mesoderm (muscles). (A) Wild type NMJ derived from larval muscle 4. (B) Reduction in NMJ size in *how24BGAL4 UAS-Smn-RNAi*^{N4}/+ animals. (C) The *how24BGAL4 UAS-Smn-RNAi*^{N4}/+ and (D) *how24BGAL4 UAS-Smn-RNAi*^{C24}/+ NMJ size defects are rescued by overexpression of Htl (*UAS-htl*^{wt}). (E) *how24BGAL4/UAS-stumps* individuals show an expansion in NMJ size. (F) The *how24BGAL4 UAS-Smn-RNAi*^{C24}/+ NMJ size defects are rescued by overexpression of Stumps (*UAS-stumps*). (G) Quantitation of bouton number/muscle in animals of different genotypes, normalized per muscle surface area (MSA) as a percentage of wild type (WT). *how24BGAL4; UASGFP* is used as control. The ANOVA multiple comparison test was used for statistical analysis of the bouton number/muscle. $P \leq 0.05$. Bar, 50 µm. $n = 40$. All preparations were stained with anti-HRP (red) and anti-Dlg (green). The muscle nucleus was labeled using DAPI.

expression impacts expression of Htl and Stumps. Using the *how24B* driver to direct expression of the *UAS-Smn-RNAi*^{N4} transgenic construct in the musculature resulted in a drastic postsynaptic reduction in Htl levels at the NMJ (Fig. 7, D–F) as well as a more general loss of Stumps staining throughout the muscle (Fig. S5). Conversely, we did not detect any obvious changes in the distribution or levels of the Smn protein when *htl* activity was reduced postsynaptically (*how24BGAL4/UAS-htl*^{DN}; Fig. 7, G–I), indicating that FGF activity does not influence *Smn* expression. These observations corroborate the relationship observed above and indicate that *Smn* regulates elements of the FGF pathway.

Ideally, the aforementioned observations, which address the issue of autonomy in the *Smn*–FGF pathway interaction, would have included data derived from classical alleles of *Smn*. Unfortunately, however, it is practically impossible to generate the motor neuron or muscle mitotic clones necessary to examine this question. For this reason, we extended our observations to include the *Drosophila* wing imaginal disc, a tissue that is well suited to this type of experiment and where the distribution and expression levels of elements of the FGF pathway have been well characterized (Sato and Kornberg, 2002). An additional benefit of analyzing this relationship in the wing disc is that it allows us to determine whether the ability of Smn to regulate Htl is not specific for the NMJ but is conserved across tissues.

Therefore, we monitored Htl and Stumps expression in *Smn* loss-of-function mitotic clones that were generated using several different classical alleles of *Smn*. In these $Smn^{-/-}$ cells, both Htl and Stumps expression were lost (Fig. 8, A–F). *htl* expression is unaffected in *stumps* mutant embryos, and conversely, *stumps* expression is unaffected in *htl* mutant embryos (Vincent et al., 1998), and we thus attribute these observations in the wing imaginal disc to the loss of *Smn* activity. Together, these results both corroborate and extend our investigation of the epistatic relationship established between *Smn* and FGF signaling.

As *Smn* is required for basic RNA metabolism, removal of its activity might be expected to affect expression of multiple proteins. Therefore, to test the specificity of the molecular relationship between *Smn* and FGF, we monitored the effects of loss of *Smn* function on the expression of F-actin and the transcription factor, Cut, a gene whose expression overlaps that of Htl in the developing wing. Our results indicate that removal of *Smn* activity had no effect on the distribution or levels of either cytoskeletal actin (Fig. 8, G–I) or Cut (not depicted) in the wing imaginal disc. Consistent with this notion, reduction of Smn at the NMJ had no discernable effect on Dlg expression (Fig. 7, D–F).

RNAi-induced knockdown of Smn affects *htl* transcript levels

Having established that reduction of Smn at the NMJ or removal of Smn activity in the wing imaginal disc reduces or eliminates Htl expression, respectively (Fig. 7 D, Fig. 8 B), indicating that the SMN–FGF relationship is not specific for the NMJ, we were

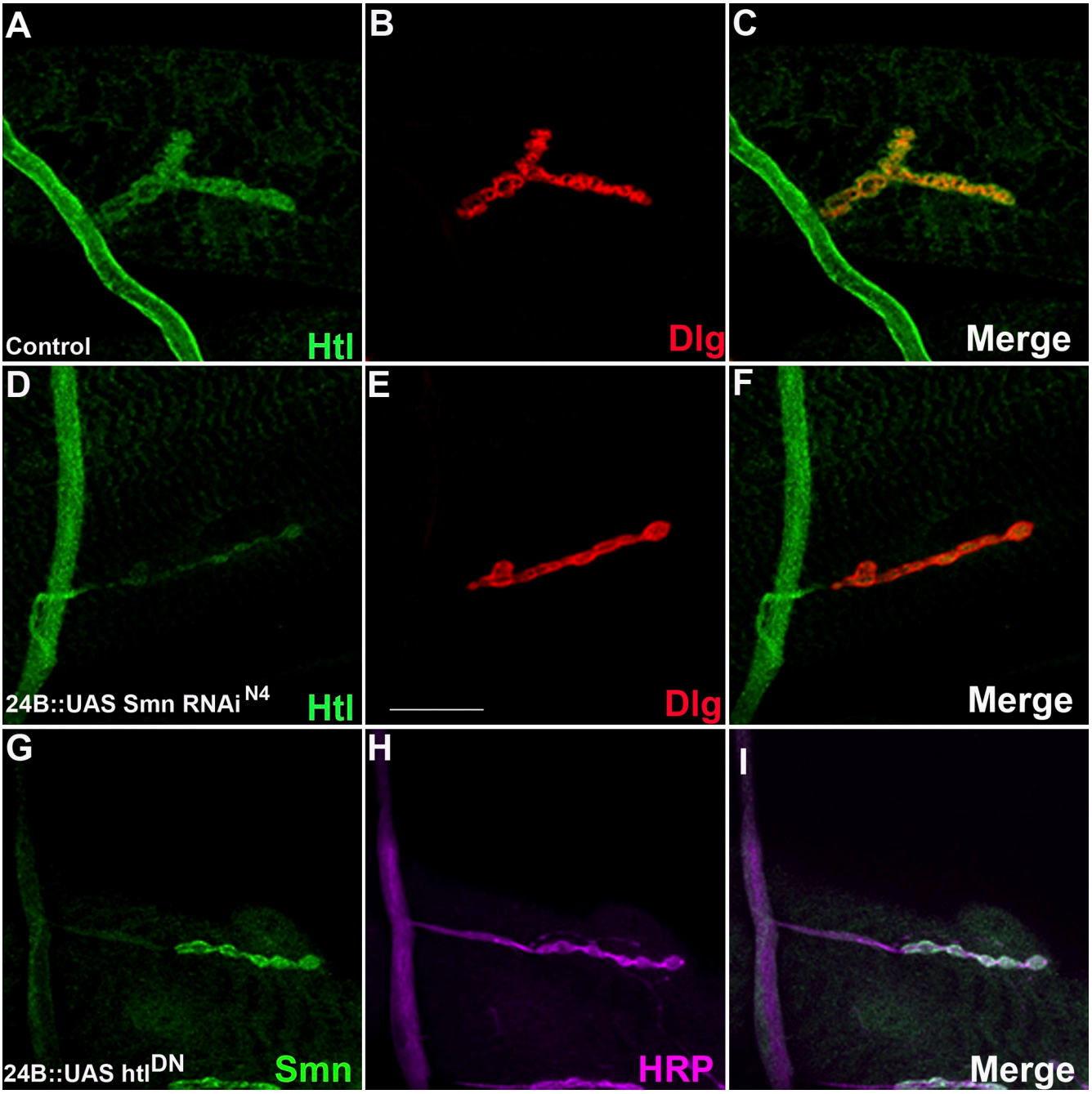

Figure 7. **Effects of *Smn* on the expression of FGF signaling pathway component at the NMJ.** All panels show NMJs derived from larval muscle 4 from wild-type (A–C) and *how24BGAL4 UAS-Smn-RNAi*^{N4}/+ (D–F) individuals. (A) Htl (green) expression is detected in the neuron as well as in the NMJ boutons. (B) Dlg (red) marks the postsynaptic region of the NMJ. (C) An overlap of A and B showing that Htl (green) expression overlaps with Dlg (red) in the postsynaptic region of the NMJ. (D) GAL4-directed muscle-specific reduction of Smn results in a loss of Htl (green) expression in postsynaptic boutons. (E) Dlg (red) marks the postsynaptic region of the NMJ. (F) An overlap of D and E showing that Htl expression is lost from the postsynaptic portion of the NMJ in a *how24BGAL4 UAS-Smn-RNAi*^{N4}/+ background. (G) Smn (green) expression in NMJ in animals expressing a dominant-negative *heartless* construct in the musculature (*how24BGAL4; UAS-htl*^{DN}). (H) The same NMJ co-stained with HRP. (I) Overlap between G and H. Bar, 50 µm. *n* = 40.

interested in exploring the underlying mechanism. Given the role of Smn in snRNP biogenesis, it is possible that reduction of Smn could alter levels of *htl* transcript, so we tested this using mRNA isolated from third larval instar brains. As shown in Fig. 8 J, knockdown of *Smn* (*tubulinGAL4::UAS-Smn-RNAi*^{FL26B}) results in *Smn* transcript levels being reduced to 16% of wild type (*tubulinGAL4*). Concomitantly, *htl* transcript is reduced to 45% of the wild-type value. Interestingly, coexpression in the aforementioned genetic background of two independent insertions of *Smn* transgenes (*UAS-Smn-FLAG*^{B} and *UAS-Smn-FLAG*^{C}) that partially rescue *Smn* lethality (Chang et al., 2008) results in slight increases in *Smn* transcripts. It is noteworthy that, depending on the construct used, we observed significantly different changes in *htl* levels. Remarkably, expression of *UAS-Smn-FLAG*^{C}, which led to only a slightly higher increase in *Smn* levels (27% of wild type) when compared with the

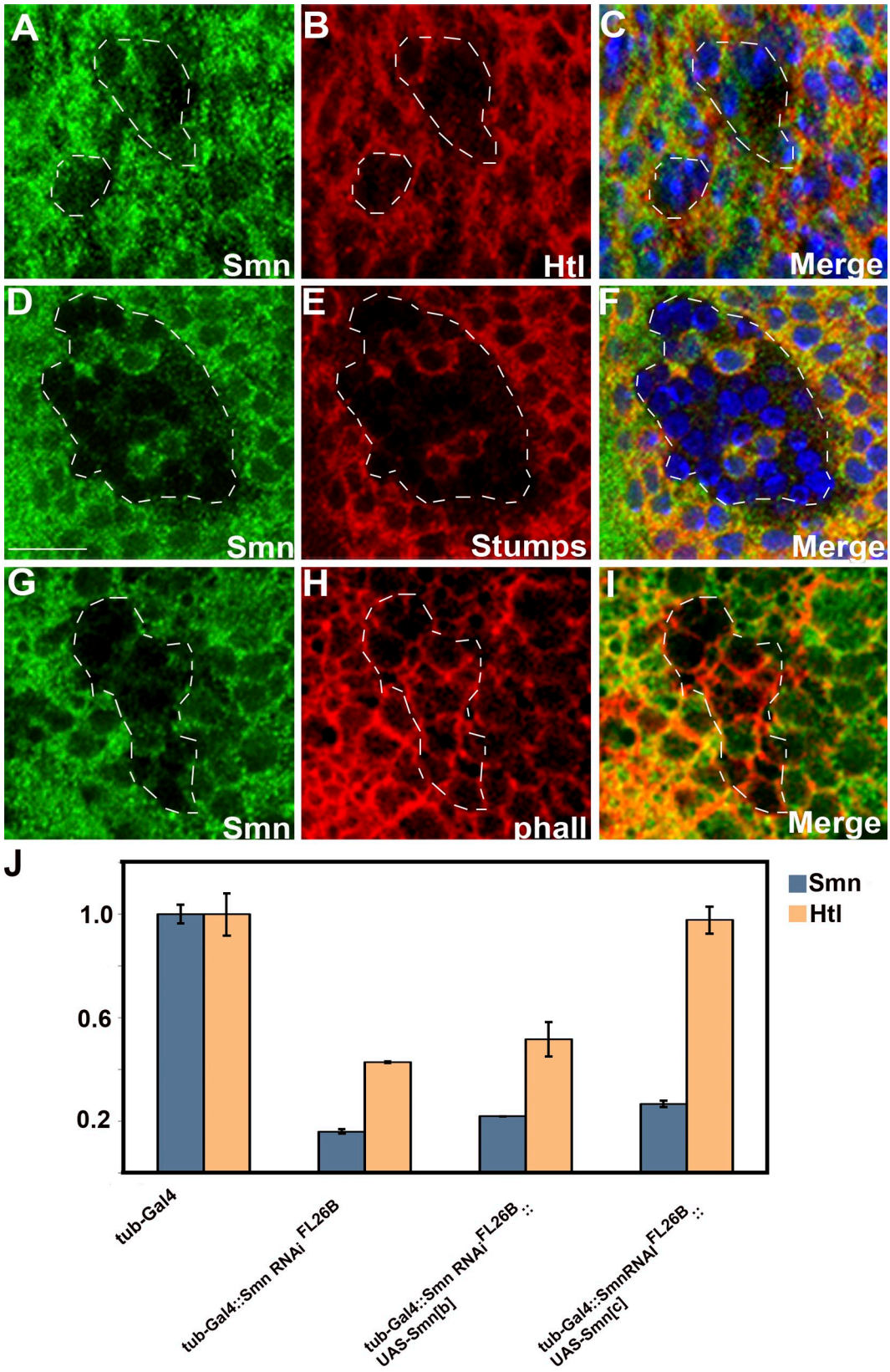

Figure 8. **Effects of *Smn* on the expression of FGF signaling pathway components in the wing disc.** (A–I) Smn^{73Ao}/Smn^{73Ao} mitotic recombination clones in third instar wing imaginal discs stained for Smn (A, D, and G), Htl (B), Stumps (E), and F-actin (H). Smn, Htl, and Stumps expression were monitored using anti-Smn (green), anti-Htl, and anti-Stumps antibodies (red). In C and F, DAPI (blue) was used to identify nuclei. Notice that Htl (B) and Stumps (E) expression is not detected in Smn^{73Ao}/Smn^{73Ao} clones, whereas removal of *Smn* activity has no effect on F-actin distribution (H). (C, F, and I) Merged images of A and B, D and E, and G and H, respectively, in which nuclei are also detected (blue). Note the presence of two Smn^{+} cells that also express Stumps are located in the center of the clone depicted in D, E, and F. (J) Quantitative RT-PCR from third instar larval brains demonstrates that altering the level of *Smn* dosage

expression of *UAS-Smn-FLAG*^{B} (21% of wild type), fully restored *htl* transcript levels to the wild-type value, as opposed to the small rescue effect we see with *UAS-Smn-FLAG*^{B}. These results demonstrate that reduction of *Smn* activity acts to modulate the levels of *htl* mRNA. Furthermore, it appears that a small increase in *Smn* may lead to a large change in the levels of *htl*, which in turn influence the survival of the animal.

Discussion

Given the variability of the SMA phenotype and the proven relationship between the severity of the disease and small changes in wild-type SMN activity, there is a significant possibility that any modifiers of SMN activity, either direct or indirect, will have therapeutic value. To systematically explore the genome for genes that are capable of modulating SMN function in vivo, we took advantage of the existence of an SMA model offered by *Drosophila* to search for *Smn* genetic interactors (Chang et al., 2008). The model we developed is based on the lethality and an associated neuromuscular junction phenotype linked to loss of *Smn* function, a phenotype remarkably similar to the NMJ phenotype reported for human patients (Kariya et al., 2008). Though the role of SMN in biogenesis of snRNPs has been well documented, its regulators and downstream effectors have not been systematically delineated, nor has the link between mutations in SMN and the specific loss of motor neurons seen in SMA patients been uncovered. It may be the case that the specificity of this phenotype is reflective of either specialized SMN functions at the NMJ or a particular sensitivity of motor neurons to the loss of SMN activity (McWhorter et al., 2003; Carrel et al., 2006; Kariya et al., 2008; Murray et al., 2008, 2010; Kong et al., 2009). Among the genes our genetic strategy revealed as *Smn* loss of function modifiers was *breathless*, encoding an FGF receptor, thus establishing a link between *Smn* and the FGF pathway (Chang et al., 2008).

Importantly, in addition to this link, we also found that FGF signaling is independently involved in NMJ morphogenesis, a function demonstrated in vertebrates (Fox et al., 2007) but not previously attributed to this pathway in *Drosophila* despite extensive characterization of its essential role in branching morphogenesis of the tracheal system, migration of multiple cell types, as well as the proper patterning of the mesoderm (Shishido et al., 1993, 1997; Beiman et al., 1996; Gisselbrecht et al., 1996; Michelson et al., 1998; Vincent et al., 1998; Schulz and Gajewski, 1999; Ghabrial et al., 2003; Stathopoulos et al., 2004). The morphological effects we observe, caused by the modulation of several pathway elements, plainly reveal an involvement of FGF signaling at the NMJ, a role confirmed by the electrophysiological analyses. The down-regulation of FGF signals in muscle results in a reduction of bouton numbers and is associated with increased mEJP amplitudes. The opposite effect is observed when FGF signaling is increased in muscles, suggesting that FGF signaling inversely regulates quantal size. Thus, FGF perturbation in muscle alters both presynaptic growth and specific aspects of synaptic transmission**.** These observations imply the existence of functional trans-synaptic homeostatic mechanisms, which have been previously shown to compensate for similar changes by increasing presynaptic bouton numbers and transmitter release (Davis et al., 1998; Sigrist et al., 2000, 2002; Menon et al., 2004). However, in this specific instance, only synaptic growth (bouton number) but not transmitter release (quantal content) is affected, the precise mechanisms for which remain unclear. Moreover, the fact that mEJP amplitudes are affected suggests that postsynaptic receptivity to glutamate release from the presynapse is altered. Similar quantal size phenotypes have been observed in several instances previously. For instance, postsynaptic PKA and NF-κB are known to regulate quantal size (Davis et al., 1998; Heckscher et al., 2007) through changes in DGluRs. Directly altering the expression of various GluR subunits also predictably influences quantal size (Petersen et al., 1997; Marrus et al., 2004; Featherstone et al., 2005). The genetic interaction we have demonstrated between FGF and *Smn* can be described as an epistatic relationship in which the FGF pathway functions downstream of *Smn* and is consistent with the observation that neuromuscular defects associated with loss of *Smn* function in muscle can be rescued by muscle-specific activation of FGF signaling. Intriguingly, the relationship we describe here between *Smn* and FGF is valid beyond the NMJ, as loss of *Smn* function genetic mosaics in the wing disc clearly result in the down-regulation of FGF signaling. Although the precise molecular mechanism underlying this relationship is still elusive, *Smn* activity affects transcript and protein levels of the FGF receptor, as well as the expression of additional elements of the FGF pathway. Whether this defines a cascade of interrelated events or whether each of these changes reflects an independent *Smn*-related regulatory event remains to be determined. Given the fact that *Smn* mutants in *Drosophila* display altered postsynaptic currents and severely compromised postsynaptic receptor clustering in muscles (Chan et al., 2003), it is conceivable that FGF signaling represents a link between *Smn* activity and postsynaptic glutamate receptor levels.

Here it should be noted that a link between SMN and the FGF pathway has been suggested by a series of studies in vertebrates where a molecular interaction between an FGF-2 isoform and the SMN protein has been described (Claus et al., 2003, 2004; Bruns et al., 2009).These studies raise the possibility that FGF-2 may negatively interfere with SMN complex function through SMN itself. Such observations would, on first appearance, suggest that the epistatic relationship between SMN and FGF signaling in vertebrate cells may be the reverse of what we observe in *Drosophila.* In point of fact however, the differences in the experimental parameters and approaches between these studies do not allow meaningful comparisons.

results in changes in *htl* transcript levels. The following genotypes are depicted: w^{1118}; *tubulinGAL4* (*tubGAL4*)/+ (columns 1 and 2), w^{1118}; *UAS-Smn-RNAi*^{FL26B}/+; *tubGAL4*/+ (columns 3 and 4), w^{1118}; *UAS-Smn-RNAi*^{FL26B}/*UAS-Smn-FLAG*^{B}; *tubGAL4*/+ (columns 5 and 6) and w^{1118}; *UAS-Smn-RNAi*^{FL26B}/+; *tubGAL4*/*UAS-Smn-FLAG*^{C} (columns 7 and 8). Levels of *Rp49* were used for normalization. Bar, 10 µm.

An important question raised by the above phenotypic analyses is whether the abnormalities associated with FGF and/or *Smn* perturbations reflect developmental or maintenance issues. It may be the case that the larval system in *Drosophila* is not ideally suited to differentiate between these alternatives as larval tissue is destined to undergo programmed cell death (histolysis) during metamorphosis. One advantage that flies do offer, however, is the ability to dissociate the development of the adult neuromuscular system from its maintenance as the entirety of its development occurs during the pupal stage, before emergence of the adult (Fernandes and Keshishian, 1998; Consoulas et al., 2002; Hebbar and Fernandes, 2004). Thus, the *Drosophila* pupa/adult may provide a platform to address these issues, as *Drosophila* displays *Smn*-dependent adult phenotypes (unpublished data; Rajendra et al., 2007). In light of the relationship we established between *Smn* and FGF signaling and the known involvement of FGF signaling in the development of both the larval and adult musculature (Emori and Saigo, 1993; Shishido et al., 1993, 1997; Vincent et al., 1998; Imam et al., 1999; Schulz and Gajewski, 1999; Stathopoulos et al., 2004; Dutta et al., 2005; Wilson et al., 2005; Kadam et al., 2009), it will be particularly interesting to examine the effects of modulating FGF activity on the aforementioned processes. Such studies may be of particular relevance to SMA where it is quite difficult to discern the developmental consequences of SMN loss in humans, as neurodegenerative symptoms displayed by patients may obscure basic problems resulting from altered developmental programs such as neuronal pathfinding, initial NMJ formation, etc (Simic et al., 2008; Liu et al., 2010).

In vertebrates, synaptic development and maintenance use at least three distinct signaling mechanisms: the TGF-β, *wingless*, and FGF pathways. In *Drosophila*, it is noteworthy that the first two have been demonstrated to function in a similar fashion at the NMJ (Packard et al., 2002; McCabe et al., 2003). Remarkably, our genetic screens involving *Smn* have identified elements of all three of these pathways as modifiers of *Smn*-related phenotypes (Chang, et al., 2008; unpublished data). We consider these connections particularly significant as they raise the possibility that *Smn* may serve as a node, integrating signaling events crucial for NMJ function, potentially leaving this structure particularly vulnerable to the loss of Smn. Though further correspondence between the *Drosophila* model and the human condition remains to be determined, the *Smn*–FGF relationship we observe in *Drosophila* raises the possibility that pharmacological manipulation of FGF signals might mitigate SMN motor neuron–related abnormalities.

Materials and methods

Drosophila stocks and culture

All fly stocks were maintained on standard fly medium at 25°C. The btl^{dev1}, htl^{AB42}, $P\{w^{+mC}=UAS\text{-}htl.DN.M\}33\text{-}B40$; $P\{w^{+mC}=UAS\text{-}htl.DN.M\}33\text{-}B61$ ($UAS\text{-}htl^{DN}$), $P\{w^{+mC}=UAS\text{-}htl.M\}YYDFR\text{-}F16$ ($UAS\text{-}htl^{wt}$), $sty^{\Delta 5}$, and sty^{226} alleles were obtained from the Bloomington *Drosophila* Stock Center (Bloomington, IN). The btl^{02864} allele was from the Exelixis collection at Harvard Medical School (Boston, MA), and the *UAS-RNAi-*btl^{27106}, *UAS-RNAi-*htl^{6692}, *UAS-RNAi-stumps*^{21317}, and *UAS-RNAi-ths*^{24536} alleles were from the Vienna *Drosophila* RNAi Center (Vienna, Austria). The *UAS-λbtl, UAS-sty,* and *UAS-stumps* (*UAS-dof*) transgenic lines were gifts from Denise Montell (Johns Hopkins University School of Medicine, Baltimore, MD; Cousins et al., 1996; Lee et al., 1996), Mark Krasnow (Stanford University School of Medicine, Stanford, CA; Sutherland et al., 1996), and Maria Leptin (European Molecular Biology Laboratory, Heidelberg, Germany; Vincent et al., 1998), respectively. *UAS-FLAG-Smn*, *UAS-Smn-RNAi*^{C24}, *UAS-Smn-RNAi*^{FL26B}, and *UAS-Smn-RNAi*^{N4} transgenic strains were used to modulate the Smn expression level (Chang et al., 2008). The *actGAL4* (Ito et al., 1997), *elavGAL4* (Luo et al., 1994), *how24B-GAL4*, *ptcGAL4* (Brand and Perrimon, 1993), and *tubGAL4* (Lee and Luo, 1999) strains were used to drive the genes placed under the UAS promoter.

Viability assay

Three driver *GAL4* males were crossed with four *UAS* transgenic females and cultured on standard fly media overnight. Flies were transferred to fresh media and allowed to lay eggs for 2 d. Adults were subsequently discarded and the progeny were cultured at 25°C. For all crosses, the percentage of viability was calculated as (1) the total number of adults divided by the total number of pupae (defined as Adults); or (2) the total number of dead pupae 4–5 d after puparium formation plus the number of individuals that reached adult stages divided by the total number of pupae (defined as Late Pupal Viability). Viability was calculated based on four independent crosses for each genotype.

Antibody staining

NMJ preparation and analysis: third instar larvae were dissected in cold 1x phosphate-buffered saline (PBS) and fixed at room temperature (RT) for 20 min in 4% paraformaldehyde (PFA). The samples were washed in 0.1% Triton X-100 in PBS (PTX) and incubated overnight at 4°C with primary antibody. The primary antibody was washed off with PTX at RT. The samples were incubated at RT with secondary antibody for 90 min. This was followed by PTX wash, and the tissues were mounted in Vectashield mounting media with DAPI (Vector Laboratories). Bouton numbers were counted using a microscope (TE2000; Nikon), based on the Discs large and anti-HRP staining in the A3 segment muscle 4 as indicated. The muscle area for every animal was measured, and no significant difference was observed among different genotypes. At least 20–25 animals of each genotype were dissected for the bouton analysis. The ANOVA multiple comparison test was used for statistical analysis of the bouton number/muscle. The images were pseudo-colored using Adobe Photoshop CS2 (v9.0.2). Wing imaginal disc preparation and analysis: third instar larvae were dissected and fixed as described previously (Kankel et al., 2004). Discs were stained at RT with the following primary antibodies in PBS Triton X-100 (PBSTx): mouse anti-Smn (Chang et al., 2008) at 1:500; rabbit anti-Htl (Shishido et al., 1997) at 1:3,000; rabbit anti-Stumps (Vincent et al., 1998) at 1:2,000; and mouse anti-Cut (Developmental Studies Hybridoma Bank) at 1:10; and were visualized with Alexa Fluor 488 goat anti–mouse (green) and Alexa Fluor 594 goat anti–rabbit (red), both at 1:1,000 (Invitrogen). Alexa Fluor 594 conjugated to phalloidin was used at 1:100 (Invitrogen). Discs were mounted in Vectashield with DAPI.

Microscopy

All images were collected with a spectral point scanning confocal (model C1si; Nikon) connected to an inverted microscope (TE2000; Nikon) equipped with DIC, phase, and epi-fluorescence optics; 40x Plan Fluor NA 1.4 objective lens; the Perfect Focus System for continuous maintenance of focus; 100-mW mercury arc lamp illumination for viewing fluorescence by eye; and confocal scanning using solid-state diode lasers (Melles Griot): 405 nm, 488 nm (10 mW), and 561 nm (10 mW). The image acquisition software used was Nikon EZ-C1. All samples were mounted and imaged in Vectashield mounting medium with DAPI (Vector Laboratories) at room temperature. Adobe Photoshop CS5 was used to pseudocolor images.

Electrophysiology

Electrophysiological recordings were made from muscle 6 in segment A3 from wandering third instar larvae in modified HL3 saline (0.5 mM Ca^{2+}) as described previously (Stewart et al., 1994; Sanyal et al., 2002; Kim et al., 2009). In brief, electrodes with tip resistances between 25–30 MΩ were used to record evoked excitatory junction potentials (EJPs) after a stimulus train delivered at 0.5 Hz to the segmental nerve such that both units were consistently recruited. Only recordings where the resting membrane potential was more polarized than −60 mV were selected for analysis. Because EJPs were larger than 10 mV in amplitude, Martin's correction for nonlinear summation was applied to all recordings (McLachlan and Martin, 1981; Kim et al., 2009). Spontaneous events (mEJPs) were recorded for a total duration of 2 min and were analyzed using MiniAnalysis

software (Synaptosoft, Inc.). EJPs were low-pass filtered and analyzed in Clampfit and representative images were generated in Microsoft Excel and Adobe Photoshop. Quantal content is determined by dividing the average corrected EJP amplitude by the average mEJP amplitude in each instance. Statistical significance was determined using ANOVA.

Strain construction

Smn FRT 79D-F chromosomes were constructed by recombining the Smn^{73Ao} (Chan et al., 2003), Smn^{f05960} (Thibault et al., 2004), and Smn^{X7} (Chang et al., 2008) alleles onto the ru^1 h^1 th^1 st^1 P{FRT(w^{hs})}2A chromosome obtained from the Bloomington Stock Center. Multiple recombinant strains for each allele were balanced using the TM6C, *Sb Tb* chromosome. Independent recombinant lines were then selected from candidate strains on the basis of a failure to complement Smn^{X7}, accompanied by loss of ru^1 h^1 th^1 st^1 markers while maintaining the *w+* expression indicative of the presence of the FRT.

Somatic mitotic clones

Clones of *Smn* tissue were induced by mitotic recombination using the FLP-FRT technique (Golic, 1991; Xu and Rubin, 1993). Mutant *Smn* clones in wing imaginal discs were identified by loss of GFP driven by the ubiquitin reporter (*Ubi*-GFP). The crosses were as follows: *y w hsFLP122; Ubi-GFP* FRT 79D-F females were crossed to Smn^{X7} FRT 79D-F/TM6C, *Sb Tb*, Smn^{73Ao} FRT 79D-F/TM6C, *Sb Tb* and Smn^{f05960} FRT 79D-F/TM6C, *Sb Tb* males. Approximately 20 *y w hsFLP122; Ubi-GFP* FRT 79D-F females were crossed to *Smn* FRT 79D-F/TM6C, *Sb Tb* males and allowed to lay eggs for 3 d at 25°C; vials were then heat-shocked at 37°C for 2 h on two consecutive days to induce somatic clones. The somatic clones produced using the Smn^{X7} allele produced very small *Smn* somatic clones and were not used for assessing Htl or Stumps expression. Smn expression was not detected in somatic clones generated using the Smn^{73Ao} allele, suggesting that it behaves as a molecular null. In Smn^{f05960} somatic clones, Smn levels were strongly reduced, but not eliminated, suggesting that it is hypomorphic in nature. Consistent with this notion, Smn and Stumps expression were reduced, but not eliminated in Smn^{f05960} somatic clones.

RNA extraction, quality control, and reverse transcription

RNA was extracted following standard procedure. In brief, third instar larvae were dissected in ice-cold PBS, and brains and wing imaginal discs (~100 brains/sample) were collected into TRIzol (Life Sciences). Samples were homogenized, and RNA was isolated after purification on an RNeasy mini column (QIAGEN). Quality control of RNA was assessed with a Bioanalyzer 2100 (Agilent Technologies) and only high quality samples were chosen for further analysis of gene expression. 200 ng of total RNA were reverse transcribed using the High Capacity RNA-to-cDNA kit (Applied Biosystems) following the manufacturer's instructions.

RT-PCR

The following oligonucleotides were designed for RT-PCR assays: *htl* sense: 5′-CGGAAGGGATCAGGATAGGG-3′ and antisense: 5′-CCTCGCCAGTCCAAAATCAG-3′; *Smn* sense: 5′-TGGGATGACTCCTTGCTGGT-3′ and antisense: 5′-GAGCAACACCTCCTGCTCGT-3′; *Rp49/RpL32* sense: 5′-CGACGCTTCAAGGGACAGTATC-3′ and antisense: 5′-TCCGACCAGGTTACAAGAACTCTC-3′.

Quantitative PCR

TaqMan gene expression assays (Applied Biosystems) were used to assess the expression of *Smn* (Dm01822923_s1) and *heartless* (Dm02373745_s1). The ribosomal protein gene *Rp49/RpL32* (Dm02151827_g1) was used as a calibrator to normalize cDNA input. 6 ng of equivalent RNA was used for each reaction and samples were processed in triplicate. To determine relative gene expression levels, data were processed using the 2^{-DDCt} method (Livak and Schmittgen, 2001) normalized to the *tub*-GAL4 control sample. All calculations and plots were generated using Excel (Microsoft).

Online supplemental material

Fig. S1 shows that Smn lethality is modified by mutations in the *Drosophila* FGF receptor breathless, and Smn knockdown alters levels of downstream targets of FGF pathway. Fig. S2 shows that postsynaptic expression of *htl RNAi* results in a loss of Htl protein localization. Fig. S3 shows bouton counts (non-normalized) of larval NMJs from genotypes depicted in Figs. 3 G, 5 G, and 6 G. Fig. S4 shows expansion of the NMJ in animals overexpressing Stumps by *how24BGAL4*. Fig. S5 shows reduction of Stumps staining in *how24BGAL4/UAS Smn RNAi*. Online supplemental material is available at http://www.jcb.org/cgi/content/full/jcb.201004016/DC1.

We thank Mark Krasnow, Maria Leptin, and Denise Montell for fly lines. The anti-Htl antibody was a gift from Testuya Kojima, and anti-Stumps antibody was a gift from Maria Leptin. This work was supported by a grant from the SMA Foundation to S. Artavanis-Tsakonas, Anne Hart, and Davie van Vactor, whom we thank for extensive input throughout the course of this work.

A. Sen was supported by a postdoctoral fellowship from the Families of Spinal Muscular Atrophy. S. Sanyal acknowledges support from grant 1R03DA027979 from the NIDA, National Institutes of Health. The authors thank the Nikon Imaging Center at Harvard Medical School for help with light microscopy.

Submitted: 2 April 2010
Accepted: 10 January 2011

References

Azzouz, M., T. Le, G.S. Ralph, L. Walmsley, U.R. Monani, D.C. Lee, F. Wilkes, K.A. Mitrophanous, S.M. Kingsman, A.H. Burghes, and N.D. Mazarakis. 2004. Lentivector-mediated SMN replacement in a mouse model of spinal muscular atrophy. *J. Clin. Invest.* 114:1726–1731.

Battle, D.J., M. Kasim, J. Yong, F. Lotti, C.K. Lau, J. Mouaikel, Z. Zhang, K. Han, L. Wan, and G. Dreyfuss. 2006. The SMN complex: an assembly machine for RNPs. *Cold Spring Harb. Symp. Quant. Biol.* 71:313–320. doi:10.1101/sqb.2006.71.001

Beiman, M., B.Z. Shilo, and T. Volk. 1996. Heartless, a *Drosophila* FGF receptor homolog, is essential for cell migration and establishment of several mesodermal lineages. *Genes Dev.* 10:2993–3002. doi:10.1101/gad.10.23.2993

Brand, A.H., and N. Perrimon. 1993. Targeted gene expression as a means of altering cell fates and generating dominant phenotypes. *Development.* 118:401–415.

Briese, M., B. Esmaeili, S. Fraboulet, E.C. Burt, S. Christodoulou, P.R. Towers, K.E. Davies, and D.B. Sattelle. 2009. Deletion of *smn-1*, the *Caenorhabditis elegans* ortholog of the spinal muscular atrophy gene, results in locomotor dysfunction and reduced lifespan. *Hum. Mol. Genet.* 18:97–104. doi:10.1093/hmg/ddn320

Bruns, A.F., J. van Bergeijk, C. Lorbeer, A. Nölle, J. Jungnickel, C. Grothe, and P. Claus. 2009. Fibroblast growth factor-2 regulates the stability of nuclear bodies. *Proc. Natl. Acad. Sci. USA.* 106:12747–12752. doi:10.1073/pnas.0900122106

Carrel, T.L., M.L. McWhorter, E. Workman, H. Zhang, E.C. Wolstencroft, C. Lorson, G.J. Bassell, A.H. Burghes, and C.E. Beattie. 2006. Survival motor neuron function in motor axons is independent of functions required for small nuclear ribonucleoprotein biogenesis. *J. Neurosci.* 26:11014–11022. doi:10.1523/JNEUROSCI.1637-06.2006

Chan, Y.B., I. Miguel-Aliaga, C. Franks, N. Thomas, B. Trülzsch, D.B. Sattelle, K.E. Davies, and M. van den Heuvel. 2003. Neuromuscular defects in a *Drosophila* survival motor neuron gene mutant. *Hum. Mol. Genet.* 12:1367–1376. doi:10.1093/hmg/ddg157

Chang, H.C., D.N. Dimlich, T. Yokokura, A. Mukherjee, M.W. Kankel, A. Sen, V. Sridhar, T.A. Fulga, A.C. Hart, D. Van Vactor, and S. Artavanis-Tsakonas. 2008. Modeling spinal muscular atrophy in *Drosophila*. *PLoS One.* 3:e3209. doi:10.1371/journal.pone.0003209

Claus, P., F. Doring, S. Gringel, F. Muller-Ostermeyer, J. Fuhlrott, T. Kraft, and C. Grothe. 2003. Differential intranuclear localization of fibroblast growth factor-2 isoforms and specific interaction with the survival of motoneuron protein. *J. Biol. Chem.* 278:479–485. doi:10.1074/jbc.M206056200

Claus, P., S. Werner, M. Timmer, and C. Grothe. 2004. Expression of the fibroblast growth factor-2 isoforms and the FGF receptor 1-4 transcripts in the rat model system of Parkinson's disease. *Neurosci. Lett.* 360:117–120. doi:10.1016/j.neulet.2004.01.046

Consoulas, C., L.L. Restifo, and R.B. Levine. 2002. Dendritic remodeling and growth of motoneurons during metamorphosis of *Drosophila melanogaster*. *J. Neurosci.* 22:4906–4917.

Cousins, D.J., D.Z. Staynov, and T.H. Lee. 1996. Regulation of cytokine genes implicated in asthma and atopy. *Monogr. Allergy.* 33:138–152.

Davis, G.W., A. DiAntonio, S.A. Petersen, and C.S. Goodman. 1998. Postsynaptic PKA controls quantal size and reveals a retrograde signal that regulates presynaptic transmitter release in *Drosophila*. *Neuron.* 20:305–315. doi:10.1016/S0896-6273(00)80458-4

Dutta, D., S. Shaw, T. Maqbool, H. Pandya, and K. Vijayraghavan. 2005. *Drosophila* Heartless acts with Heartbroken/Dof in muscle founder differentiation. *PLoS Biol.* 3:e337. doi:10.1371/journal.pbio.0030337

Eggert, C., A. Chari, B. Laggerbauer, and U. Fischer. 2006. Spinal muscular atrophy: the RNP connection. *Trends Mol. Med.* 12:113–121. doi:10.1016/j.molmed.2006.01.005

Emori, Y., and K. Saigo. 1993. Distinct expression of two *Drosophila* homologs of fibroblast growth factor receptors in imaginal discs. *FEBS Lett.* 332:111–114. doi:10.1016/0014-5793(93)80494-F

Featherstone, D.E., E. Rushton, J. Rohrbough, F. Liebl, J. Karr, Q. Sheng, C.K. Rodesch, and K. Broadie. 2005. An essential *Drosophila* glutamate receptor subunit that functions in both central neuropil and neuromuscular junction. *J. Neurosci.* 25:3199–3208. doi:10.1523/JNEUROSCI.4201-04.2005

Fernandes, J.J., and H. Keshishian. 1998. Nerve-muscle interactions during flight muscle development in *Drosophila*. *Development.* 125:1769–1779.

Forni, J.J., S. Romani, P. Doherty, and G. Tear. 2004. Neuroglian and FasciclinII can promote neurite outgrowth via the FGF receptor Heartless. *Mol. Cell. Neurosci.* 26:282–291. doi:10.1016/j.mcn.2004.02.003

Fox, M.A., J.R. Sanes, D.B. Borza, V.P. Eswarakumar, R. Fässler, B.G. Hudson, S.W. John, Y. Ninomiya, V. Pedchenko, S.L. Pfaff, et al. 2007. Distinct target-derived signals organize formation, maturation, and maintenance of motor nerve terminals. *Cell.* 129:179–193. doi:10.1016/j.cell.2007.02.035

Frugier, T., F.D. Tiziano, C. Cifuentes-Diaz, P. Miniou, N. Roblot, A. Dierich, M. Le Meur, and J. Melki. 2000. Nuclear targeting defect of SMN lacking the C-terminus in a mouse model of spinal muscular atrophy. *Hum. Mol. Genet.* 9:849–858. doi:10.1093/hmg/9.5.849

García-Alonso, L., S. Romani, and F. Jiménez. 2000. The EGF and FGF receptors mediate neuroglian function to control growth cone decisions during sensory axon guidance in *Drosophila*. *Neuron.* 28:741–752. doi:10.1016/S0896-6273(00)00150-1

Ghabrial, A., S. Luschnig, M.M. Metzstein, and M.A. Krasnow. 2003. Branching morphogenesis of the *Drosophila* tracheal system. *Annu. Rev. Cell Dev. Biol.* 19:623–647. doi:10.1146/annurev.cellbio.19.031403.160043

Gisselbrecht, S., J.B. Skeath, C.Q. Doe, and A.M. Michelson. 1996. heartless encodes a fibroblast growth factor receptor (DFR1/DFGF-R2) involved in the directional migration of early mesodermal cells in the *Drosophila* embryo. *Genes Dev.* 10:3003–3017. doi:10.1101/gad.10.23.3003

Glazer, L., and B.Z. Shilo. 1991. The *Drosophila* FGF-R homolog is expressed in the embryonic tracheal system and appears to be required for directed tracheal cell extension. *Genes Dev.* 5:697–705. doi:10.1101/gad.5.4.697

Golic, K.G. 1991. Site-specific recombination between homologous chromosomes in *Drosophila*. *Science.* 252:958–961. doi:10.1126/science.2035025

Hannus, S., D. Bühler, M. Romano, B. Seraphin, and U. Fischer. 2000. The *Schizosaccharomyces pombe* protein Yab8p and a novel factor, Yip1p, share structural and functional similarity with the spinal muscular atrophy-associated proteins SMN and SIP1. *Hum. Mol. Genet.* 9:663–674. doi:10.1093/hmg/9.5.663

Hebbar, S., and J.J. Fernandes. 2004. Pruning of motor neuron branches establishes the DLM innervation pattern in *Drosophila*. *J. Neurobiol.* 60:499–516. doi:10.1002/neu.20031

Heckscher, E.S., R.D. Fetter, K.W. Marek, S.D. Albin, and G.W. Davis. 2007. NF-kappaB, IkappaB, and IRAK control glutamate receptor density at the *Drosophila* NMJ. *Neuron.* 55:859–873. doi:10.1016/j.neuron.2007.08.005

Hsieh-Li, H.M., J.G. Chang, Y.J. Jong, M.H. Wu, N.M. Wang, C.H. Tsai, and H. Li. 2000. A mouse model for spinal muscular atrophy. *Nat. Genet.* 24:66–70. doi:10.1038/71709

Huang, P., and M.J. Stern. 2005. FGF signaling in flies and worms: more and more relevant to vertebrate biology. *Cytokine Growth Factor Rev.* 16:151–158. doi:10.1016/j.cytogfr.2005.03.002

Imam, F., D. Sutherland, W. Huang, and M.A. Krasnow. 1999. *stumps*, a *Drosophila* gene required for fibroblast growth factor (FGF)-directed migrations of tracheal and mesodermal cells. *Genetics.* 152:307–318.

Ito, K., W. Awano, K. Suzuki, Y. Hiromi, and D. Yamamoto. 1997. The *Drosophila* mushroom body is a quadruple structure of clonal units each of which contains a virtually identical set of neurones and glial cells. *Development.* 124:761–771.

Itoh, N., and D.M. Ornitz. 2004. Evolution of the Fgf and Fgfr gene families. *Trends Genet.* 20:563–569. doi:10.1016/j.tig.2004.08.007

Jarvis, L.A., S.J. Toering, M.A. Simon, M.A. Krasnow, and R.K. Smith-Bolton. 2006. Sprouty proteins are in vivo targets of Corkscrew/SHP-2 tyrosine phosphatases. *Development.* 133:1133–1142. doi:10.1242/dev.02255

Kadam, S., A. McMahon, P. Tzou, and A. Stathopoulos. 2009. FGF ligands in *Drosophila* have distinct activities required to support cell migration and differentiation. *Development.* 136:739–747. doi:10.1242/dev.027904

Kankel, M.W., D.M. Duncan, and I. Duncan. 2004. A screen for genes that interact with the *Drosophila* pair-rule segmentation gene fushi tarazu. *Genetics.* 168:161–180. doi:10.1534/genetics.104.027250

Kariya, S., G.H. Park, Y. Maeno-Hikichi, O. Leykekhman, C. Lutz, M.S. Arkovitz, L.T. Landmesser, and U.R. Monani. 2008. Reduced SMN protein impairs maturation of the neuromuscular junctions in mouse models of spinal muscular atrophy. *Hum. Mol. Genet.* 17:2552–2569. doi:10.1093/hmg/ddn156

Kerr, D.A., J. Lladó, M.J. Shamblott, N.J. Maragakis, D.N. Irani, T.O. Crawford, C. Krishnan, S. Dike, J.D. Gearhart, and J.D. Rothstein. 2003. Human embryonic germ cell derivatives facilitate motor recovery of rats with diffuse motor neuron injury. *J. Neurosci.* 23:5131–5140.

Kim, S.M., V. Kumar, Y.Q. Lin, S. Karunanithi, and M. Ramaswami. 2009. Fos and Jun potentiate individual release sites and mobilize the reserve synaptic vesicle pool at the *Drosophila* larval motor synapse. *Proc. Natl. Acad. Sci. USA.* 106:4000–4005. doi:10.1073/pnas.0806064106

Kong, L., X. Wang, D.W. Choe, M. Polley, B.G. Burnett, M. Bosch-Marcé, J.W. Griffin, M.M. Rich, and C.J. Sumner. 2009. Impaired synaptic vesicle release and immaturity of neuromuscular junctions in spinal muscular atrophy mice. *J. Neurosci.* 29:842–851. doi:10.1523/JNEUROSCI.4434-08.2009

Lee, T., and L. Luo. 1999. Mosaic analysis with a repressible cell marker for studies of gene function in neuronal morphogenesis. *Neuron.* 22:451–461. doi:10.1016/S0896-6273(00)80701-1

Lee, T., N. Hacohen, M. Krasnow, and D.J. Montell. 1996. Regulated Breathless receptor tyrosine kinase activity required to pattern cell migration and branching in the *Drosophila* tracheal system. *Genes Dev.* 10:2912–2921. doi:10.1101/gad.10.22.2912

Lefebvre, S., P. Burlet, Q. Liu, S. Bertrandy, O. Clermont, A. Munnich, G. Dreyfuss, and J. Melki. 1997. Correlation between severity and SMN protein level in spinal muscular atrophy. *Nat. Genet.* 16:265–269. doi:10.1038/ng0797-265

Liu, H., D. Shafey, J.N. Moores, and R. Kothary. 2010. Neurodevelopmental consequences of Smn depletion in a mouse model of spinal muscular atrophy. *J. Neurosci. Res.* 88:111–122. doi:10.1002/jnr.22189

Liu, J.L., C. Murphy, M. Buszczak, S. Clatterbuck, R. Goodman, and J.G. Gall. 2006. The *Drosophila melanogaster* Cajal body. *J. Cell Biol.* 172:875–884. doi:10.1083/jcb.200511038

Livak, K.J., and T.D. Schmittgen. 2001. Analysis of relative gene expression data using real-time quantitative PCR and the 2(-Delta Delta C(T)) Method. *Methods*. 25:402–408. doi:10.1006/meth.2001.1262

Luo, L., Y.J. Liao, L.Y. Jan, and Y.N. Jan. 1994. Distinct morphogenetic functions of similar small GTPases: *Drosophila* Drac1 is involved in axonal outgrowth and myoblast fusion. *Genes Dev.* 8:1787–1802. doi:10.1101/gad.8.15.1787

Marrus, S.B., S.L. Portman, M.J. Allen, K.G. Moffat, and A. DiAntonio. 2004. Differential localization of glutamate receptor subunits at the *Drosophila* neuromuscular junction. *J. Neurosci.* 24:1406–1415. doi:10.1523/JNEUROSCI.1575-03.2004

Massenet, S., L. Pellizzoni, S. Paushkin, I.W. Mattaj, and G. Dreyfuss. 2002. The SMN complex is associated with snRNPs throughout their cytoplasmic assembly pathway. *Mol. Cell. Biol.* 22:6533–6541. doi:10.1128/MCB.22.18.6533-6541.2002

McAndrew, P.E., D.W. Parsons, L.R. Simard, C. Rochette, P.N. Ray, J.R. Mendell, T.W. Prior, and A.H. Burghes. 1997. Identification of proximal spinal muscular atrophy carriers and patients by analysis of SMNT and SMNC gene copy number. *Am. J. Hum. Genet.* 60:1411–1422. doi:10.1086/515465

McCabe, B.D., G. Marqués, A.P. Haghighi, R.D. Fetter, M.L. Crotty, T.E. Haerry, C.S. Goodman, and M.B. O'Connor. 2003. The BMP homolog Gbb provides a retrograde signal that regulates synaptic growth at the *Drosophila* neuromuscular junction. *Neuron*. 39:241–254. doi:10.1016/S0896-6273(03)00426-4

McLachlan, E.M., and A.R. Martin. 1981. Non-linear summation of end-plate potentials in the frog and mouse. *J. Physiol.* 311:307–324.

McWhorter, M.L., U.R. Monani, A.H. Burghes, and C.E. Beattie. 2003. Knockdown of the survival motor neuron (Smn) protein in zebrafish causes defects in motor axon outgrowth and pathfinding. *J. Cell Biol.* 162:919–931. doi:10.1083/jcb.200303168

Meister, G., C. Eggert, and U. Fischer. 2002. SMN-mediated assembly of RNPs: a complex story. *Trends Cell Biol.* 12:472–478. doi:10.1016/S0962-8924(02)02371-1

Menon, K.P., S. Sanyal, Y. Habara, R. Sanchez, R.P. Wharton, M. Ramaswami, and K. Zinn. 2004. The translational repressor Pumilio regulates presynaptic morphology and controls postsynaptic accumulation of translation factor eIF-4E. *Neuron.* 44:663–676. doi:10.1016/j.neuron.2004.10.028

Michelson, A.M., S. Gisselbrecht, Y. Zhou, K.H. Baek, and E.M. Buff. 1998. Dual functions of the heartless fibroblast growth factor receptor in development of the *Drosophila* embryonic mesoderm. *Dev. Genet.* 22:212–229. doi:10.1002/(SICI)1520-6408(1998)22:3<212::AID-DVG4>3.0.CO;2-9

Miguel-Aliaga, I., E. Culetto, D.S. Walker, H.A. Baylis, D.B. Sattelle, and K.E. Davies. 1999. The Caenorhabditis elegans orthologue of the human gene responsible for spinal muscular atrophy is a maternal product critical for germline maturation and embryonic viability. *Hum. Mol. Genet.* 8:2133–2143. doi:10.1093/hmg/8.12.2133

Miguel-Aliaga, I., Y.B. Chan, K.E. Davies, and M. van den Heuvel. 2000. Disruption of SMN function by ectopic expression of the human SMN gene in *Drosophila*. *FEBS Lett.* 486:99–102. doi:10.1016/S0014-5793(00)02243-2

Monani, U.R. 2005. Spinal muscular atrophy: a deficiency in a ubiquitous protein; a motor neuron-specific disease. *Neuron.* 48:885–896. doi:10.1016/j.neuron.2005.12.001

Monani, U.R., M. Sendtner, D.D. Coovert, D.W. Parsons, C. Andreassi, T.T. Le, S. Jablonka, B. Schrank, W. Rossoll, T.W. Prior, et al. 2000. The human centromeric survival motor neuron gene (SMN2) rescues embryonic lethality in Smn(−/−) mice and results in a mouse with spinal muscular atrophy. *Hum. Mol. Genet.* 9:333–339. doi:10.1093/hmg/9.3.333

Murray, L.M., L.H. Comley, D. Thomson, N. Parkinson, K. Talbot, and T.H. Gillingwater. 2008. Selective vulnerability of motor neurons and dissociation of pre- and post-synaptic pathology at the neuromuscular junction in mouse models of spinal muscular atrophy. *Hum. Mol. Genet.* 17:949–962. doi:10.1093/hmg/ddm367

Murray, L.M., S. Lee, D. Bäumer, S.H. Parson, K. Talbot, and T.H. Gillingwater. 2010. Pre-symptomatic development of lower motor neuron connectivity in a mouse model of severe spinal muscular atrophy. *Hum. Mol. Genet.* 19:420–433. doi:10.1093/hmg/ddp506

Owen, N., C.L. Doe, J. Mellor, and K.E. Davies. 2000. Characterization of the *Schizosaccharomyces pombe* orthologue of the human survival motor neuron (SMN) protein. *Hum. Mol. Genet.* 9:675–684. doi:10.1093/hmg/9.5.675

Packard, M., E.S. Koo, M. Gorczyca, J. Sharpe, S. Cumberledge, and V. Budnik. 2002. The *Drosophila* Wnt, wingless, provides an essential signal for pre- and postsynaptic differentiation. *Cell.* 111:319–330. doi:10.1016/S0092-8674(02)01047-4

Paushkin, S., B. Charroux, L. Abel, R.A. Perkinson, L. Pellizzoni, and G. Dreyfuss. 2000. The survival motor neuron protein of *Schizosaccharomyces pombe*. Conservation of survival motor neuron interaction domains in divergent organisms. *J. Biol. Chem.* 275:23841–23846. doi:10.1074/jbc.M001441200

Paushkin, S., A.K. Gubitz, S. Massenet, and G. Dreyfuss. 2002. The SMN complex, an assemblyosome of ribonucleoproteins. *Curr. Opin. Cell Biol.* 14:305–312. doi:10.1016/S0955-0674(02)00332-0

Petersen, S.A., R.D. Fetter, J.N. Noordermeer, C.S. Goodman, and A. DiAntonio. 1997. Genetic analysis of glutamate receptors in *Drosophila* reveals a retrograde signal regulating presynaptic transmitter release. *Neuron.* 19:1237–1248. doi:10.1016/S0896-6273(00)80415-8

Petit, V., U. Nussbaumer, C. Dossenbach, and M. Affolter. 2004. Downstream-of-FGFR is a fibroblast growth factor-specific scaffolding protein and recruits Corkscrew upon receptor activation. *Mol. Cell. Biol.* 24:3769–3781. doi:10.1128/MCB.24.9.3769-3781.2004

Rajendra, T.K., G.B. Gonsalvez, M.P. Walker, K.B. Shpargel, H.K. Salz, and A.G. Matera. 2007. A *Drosophila melanogaster* model of spinal muscular atrophy reveals a function for SMN in striated muscle. *J. Cell Biol.* 176:831–841. doi:10.1083/jcb.200610053

Sanyal, S., D.J. Sandstrom, C.A. Hoeffer, and M. Ramaswami. 2002. AP-1 functions upstream of CREB to control synaptic plasticity in *Drosophila*. *Nature.* 416:870–874. doi:10.1038/416870a

Sato, M., and T.B. Kornberg. 2002. FGF is an essential mitogen and chemoattractant for the air sacs of the *Drosophila* tracheal system. *Dev. Cell.* 3:195–207. doi:10.1016/S1534-5807(02)00202-2

Schrank, B., R. Götz, J.M. Gunnersen, J.M. Ure, K.V. Toyka, A.G. Smith, and M. Sendtner. 1997. Inactivation of the survival motor neuron gene, a candidate gene for human spinal muscular atrophy, leads to massive cell death in early mouse embryos. *Proc. Natl. Acad. Sci. USA.* 94:9920–9925. doi:10.1073/pnas.94.18.9920

Schulz, R.A., and K. Gajewski. 1999. Ventral neuroblasts and the heartless FGF receptor are required for muscle founder cell specification in *Drosophila*. *Oncogene.* 18:6818–6823. doi:10.1038/sj.onc.1203081

Shishido, E., S. Higashijima, Y. Emori, and K. Saigo. 1993. Two FGF-receptor homologues of *Drosophila*: one is expressed in mesodermal primordium in early embryos. *Development.* 117:751–761.

Shishido, E., N. Ono, T. Kojima, and K. Saigo. 1997. Requirements of DFR1/Heartless, a mesoderm-specific *Drosophila* FGF-receptor, for the formation of heart, visceral and somatic muscles, and ensheathing of longitudinal axon tracts in CNS. *Development.* 124:2119–2128.

Sigrist, S.J., P.R. Thiel, D.F. Reiff, P.E. Lachance, P. Lasko, and C.M. Schuster. 2000. Postsynaptic translation affects the efficacy and morphology of neuromuscular junctions. *Nature.* 405:1062–1065. doi:10.1038/35016598

Sigrist, S.J., P.R. Thiel, D.F. Reiff, and C.M. Schuster. 2002. The postsynaptic glutamate receptor subunit DGluR-IIA mediates long-term plasticity in *Drosophila*. *J. Neurosci.* 22:7362–7372.

Simic, G., M. Mladinov, D. Seso Simic, N. Jovanov Milosevic, A. Islam, A. Pajtak, N. Barisic, J. Sertic, P.J. Lucassen, P.R. Hof, and B. Kruslin. 2008. Abnormal motoneuron migration, differentiation, and axon outgrowth in spinal muscular atrophy. *Acta Neuropathol.* 115:313–326. doi:10.1007/s00401-007-0327-1

Stathopoulos, A., B. Tam, M. Ronshaugen, M. Frasch, and M. Levine. 2004. pyramus and thisbe: FGF genes that pattern the mesoderm of *Drosophila* embryos. *Genes Dev.* 18:687–699. doi:10.1101/gad.1166404

Stewart, B.A., H.L. Atwood, J.J. Renger, J. Wang, and C.F. Wu. 1994. Improved stability of *Drosophila* larval neuromuscular preparations in haemolymph-like physiological solutions. *J. Comp. Physiol. [A].* 175:179–191. doi:10.1007/BF00215114

Sutherland, D., C. Samakovlis, and M.A. Krasnow. 1996. branchless encodes a *Drosophila* FGF homolog that controls tracheal cell migration and the pattern of branching. *Cell.* 87:1091–1101. doi:10.1016/S0092-8674(00)81803-6

Thibault, S.T., M.A. Singer, W.Y. Miyazaki, B. Milash, N.A. Dompe, C.M. Singh, R. Buchholz, M. Demsky, R. Fawcett, H.L. Francis-Lang, et al. 2004. A complementary transposon tool kit for *Drosophila melanogaster* using P and piggyBac. *Nat. Genet.* 36:283–287. doi:10.1038/ng1314

Vincent, S., R. Wilson, C. Coelho, M. Affolter, and M. Leptin. 1998. The *Drosophila* protein Dof is specifically required for FGF signaling. *Mol. Cell.* 2:515–525. doi:10.1016/S1097-2765(00)80151-3

Wan, L., D.J. Battle, J. Yong, A.K. Gubitz, S.J. Kolb, J. Wang, and G. Dreyfuss. 2005. The survival of motor neurons protein determines the capacity for snRNP assembly: biochemical deficiency in spinal muscular atrophy. *Mol. Cell. Biol.* 25:5543–5551. doi:10.1128/MCB.25.13.5543-5551.2005

Wilson, R., E. Vogelsang, and M. Leptin. 2005. FGF signalling and the mechanism of mesoderm spreading in *Drosophila* embryos. *Development.* 132:491–501. doi:10.1242/dev.01603

Wolstencroft, E.C., V. Mattis, A.A. Bajer, P.J. Young, and C.L. Lorson. 2005. A non-sequence-specific requirement for SMN protein activity: the role of aminoglycosides in inducing elevated SMN protein levels. *Hum. Mol. Genet.* 14:1199–1210. doi:10.1093/hmg/ddi131

Xu, T., and G.M. Rubin. 1993. Analysis of genetic mosaics in developing and adult *Drosophila* tissues. *Development.* 117:1223–1237.

Zhang, Z., F. Lotti, K. Dittmar, I. Younis, L. Wan, M. Kasim, and G. Dreyfuss. 2008. SMN deficiency causes tissue-specific perturbations in the repertoire of snRNAs and widespread defects in splicing. *Cell.* 133:585–600. doi:10.1016/j.cell.2008.03.031